Are the available data from laboratory spray burners suitable for CFD modelling validations? A review

Brito Lopes, A. V., Emekwuru, N. & Joshi, K.

DOI 10.1016/j.ecmx.2022.100289
ISSN 2590-1745

Publisher: Elsevier

Energy Conversion and Management: X 16 (2022) 100289

Contents lists available at ScienceDirect

Energy Conversion and Management: X

journal homepage: www.sciencedirect.com/journal/energy-conversion-and-management-x

Are the available data from laboratory spray burners suitable for CFD modelling validations? A review

A.V. Brito Lopes [a,*], N. Emekwuru [b,c,*], K. Joshi [c]

[a] Centre for Fluid and Complex Systems, Coventry University, Coventry CV1 5FB, UK
[b] Institute for Future Transport and Cities, Coventry University, Coventry CV1 5FB, UK
[c] Faculty of Engineering, Environment & Computing, Coventry University, Coventry CV1 5FB, UK

ARTICLE INFO

Keywords:
Highly-swirling-turbulent-spray-flame-combustion
Laboratory-scale-spray-burners
Computational-fluid-dynamics
Non-reacting-flows
Validation-database
Future fuels
Gas-turbines

ABSTRACT

A systematic compilation and evaluation of turbulent spray flame combustion data acquired from lab-scale spray-burners and CFD models validated with these are presented. Previous review studies have been limited to presentations of the progress with validation targets and modelling methods. This work expands these by presenting the details of lab-scale spray-burners and the characteristics of their datasets, the computational methodologies developed to capture the turbulent spray combustion processes acquired from the burners and their validation with the dataset. Additionally, by critically evaluating the spray and inflow boundary conditions, the reacting and non-reacting features and the main flame characteristics and data, direct correlations between the effectiveness of the dataset from the lab-scale spray burners and the outcomes from the computational methodologies using them for validation are clearly elucidated. The evaluation indicates that the turbulence modelling and validation of the swirling non-reacting flows before the application of the combustion models are important. A better representation of the multi-mode nature and the flame-turbulence-chemistry interactions in the combustion models are required. Also, a clearer experimental presentation of the flame structure and modes would help with the development of the modelling techniques. To plug these research needs, this paper reinforces the importance of developing improved numerical techniques that can be validated by selecting an appropriate lab-scale spray-burner with a robust database. Together these can be used to improve the development of and reduce emissions from combustors burning future green fuels.

Introduction

The aircraft industry relies on the consumption of liquid fossil-fuels, which are experiencing cost increases due to resource constraints. The industry is also drawing attention due to worldwide concerns regarding greenhouse gas carbon dioxide (CO_2), nitric oxide (NO_x), sulphur oxides (SO_x) and soot emissions. For example, there is evidence that CO_2 emissions have increased by 3 % per year between 1990 and 2010 and keep growing Intergovernmental Panel on Climate Change [51]. The Committee on Aviation Environmental Protection of the International Civil Aviation Organisation (ICAO) argues that technological and operational improvements must be made to reduce CO_2 emissions; otherwise, emissions might be up to be seven times higher in 2050 than it used to be in 1990. Under such considerations, the move towards Sustainable Aviation Fuel (SAF) and the development of more efficient combustion systems can aid in the reduction of greenhouse emissions and the consumption of fossil fuels, therefore, contributing to a more neutral CO_2 footprint. Thus, it is a current topic of immense scientific interest.

Given the situation as noted above, the studies of the atomisation and combustion of liquid fuels, in reciprocating engines, rockets, and aircraft gas-turbines, so as to reduce fuel consumption and emissions, have taken more prominence. However, the studies are not inconsequential as turbulent spray flames of liquid-fuels are characterised by several complex physics phenomena involving the spray flame. For application in aero-gas turbines, the liquid-fuel requires a mechanism of injection that provides a high level of fuel atomisation (usually achieved using air-blast injectors or air-assisted injectors) and an entrance air co-flow with enough swirling motion to promote a central recirculation zone that is responsible for aiding the fuel and air mixing and flame stabilisation [11], Brito Lopes [10], Brito Lopes et al. [12]. This can result in a compact and stable reaction area, combustion rate increases (since hot

* Correspondence authors at: Institute for Future Transport and Cities, Coventry University, Coventry CV1 5FB, UK
E-mail addresses: britoloa@uni.coventry.ac.uk (A.V. Brito Lopes), ab9992@coventry.ac.uk (N. Emekwuru), kruti1996@outlook.com (K. Joshi).

https://doi.org/10.1016/j.ecmx.2022.100289
Received 23 May 2022; Received in revised form 12 August 2022; Accepted 23 August 2022
Available online 29 August 2022

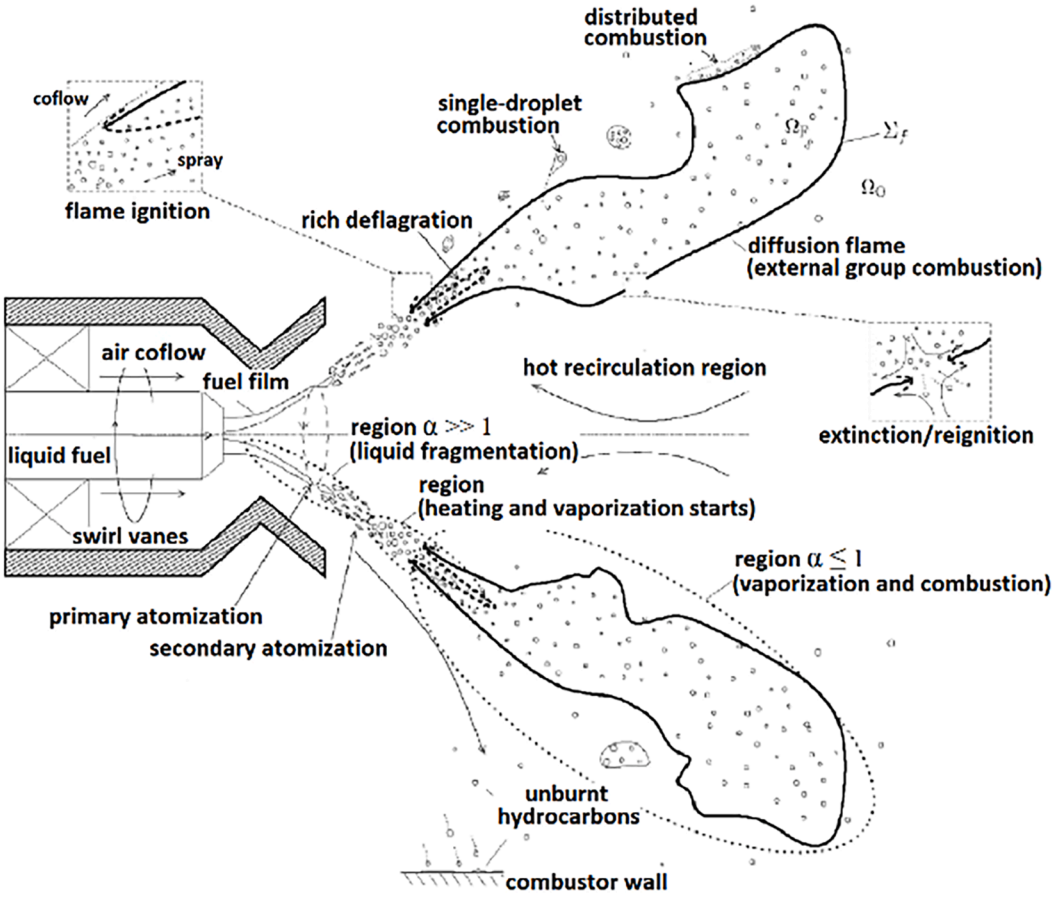

Fig. 1-1. Spray combustion processes in a continuous-combustion system. α = mass-loading and represents the ratio of the mass of the droplet to the mass of the corresponding surrounding gas Sánchez et al. [133].

recirculation air keeps feeding the flame root) and, thus, the required combustion chamber volume could be less hence improving the aircraft power-to-weight ratio [74], Lieuwen [77] and Lefebvre and Ballal [75].

An example of the complex physical nature involved in a turbulent spray flame is depicted in Fig. 1-1. In the primary atomisation zone, there is a high concentration of droplets which has a slow vaporisation process. Then, due to the high swirl effects, the cold liquid starts its fragmentation (in a region of the rich mixture). The secondary atomisation takes place, followed by the heating and vaporisation of droplets, which relies on the sensible heat of the surrounding recirculated hot gases and vaporisation. A premixed rich flame is generated during this stage. Once the atomisation process is fully developed, droplet dispersion becomes very large, increasing the surface area, and the main diffusion flame appears in the vaporisation region.

Motivation for a new literature review

There are few studies such as Hochgreb [46] and Giusti and Mastorakos [40] covering the physical phenomena of flames on both gaseous and spray laboratory-scale burners. The Hochgreb [46] study concentrated on the validation targets and methods for turbulent combustion models, whilst Giusti and Mastorakos [40] presented the progress in the modelling of the finite-rate effects in turbulent combustion, presented the trends in laboratory studies and discussed how international combustion networks had contributed to the field. However, to our knowledge, review studies presenting the details of the experimental configurations/datasets *and* the computational methodologies for turbulent spray combustion whilst establishing a direct correlation between the effectiveness of the experimental dataset and the outcomes achieved from the Computational Fluid Dynamics (CFD) simulations are lacking, hence making it difficult to correlate the deficiencies of the CFD models. The potential of the datasets derived from the laboratory scale burners in generating reliable boundary conditions (BCs) for the CFD models and, therefore, the establishment and assessment of these BCs on the CFD modelling have been marginally explored in previous literature.

This review addresses the above gaps. The efficacy of various CFD numerical modelling results are directly correlated with the experimental results that are used to validate the CFD results and these are discussed in detail. The fundamental issues regarding the efficacy of boundary conditions generated from experimental datasets are presented and discussed. Particular attention is paid to the validation processes involving the modelling of cold-reacting flows, which are precursor simulations of reacting cases. For spray combustion CFD modellers, this review offers data that will enable them to decide which burner to use based on understanding the burners' operational features, the experimental dataset available, and the issues that may arise due to the boundary conditions data available. Gaps in the capabilities of the CFD models assessed in section Computational modelling and potential directions for modelling improvements are also presented. Experimentalists will have access to a compilation of spray burners, their experimental techniques, their limitations, and how useful their data are to CFD studies.

Objectives

The main goals of this study are twofold; firstly, to present an overview of relevant experimental work on laboratory spray burners that can be used as databases for numerical modelling development and

validation. Detailed descriptions of the experimental setup (design and construction), the main features of the burners in terms of the flame physics investigated and the major measured data for both non-reacting and reacting flows are presented and assessed. Particular attention is devoted to analysing the potential of the presented database for use in CFD simulations. Secondly, an overview of the current state-of-the-art CFD modelling techniques applied to the data from such burners are presented and discussed in order to identify their main limitations and explore the directions for improvement. Therefore, the reader can directly correlate the experimental data for such burners with the efficacy of the numerical techniques used to predict them.

Considering the extensive nature of the field of spray combustion and all the research carried out so far, the scope of this paper is further narrowed down. Only laboratory-scale burners (either in swirling or non-swirling environments), for confined and unconfined cases, using atomized liquid-fuels relevant to the development of aero-gas engines are assessed and considered in the review. Therefore, the burners considered have included these features:

I. Detailed information on the geometry, the measurements of non-reacting flow in terms of time-averaged and fluctuating velocity fields (hence allowing for the numerical characterisation of the influence of the processing vortex core, vortex breakdown and recirculation zones) for the swirling case, and on the well-established inlet boundary conditions for both the non-reacting and the reacting flows,
II. Detailed data of the optical measurements of the flame structure visualisation and relevant scalars measurements for flame characterisation, combined measurement techniques that allow for a better understanding of the turbulence-chemistry interactions as well as the validation of spray/droplets evaporation, and
III. The use of alternative fuels such as biofuels due to their relevance for emissions mitigation.

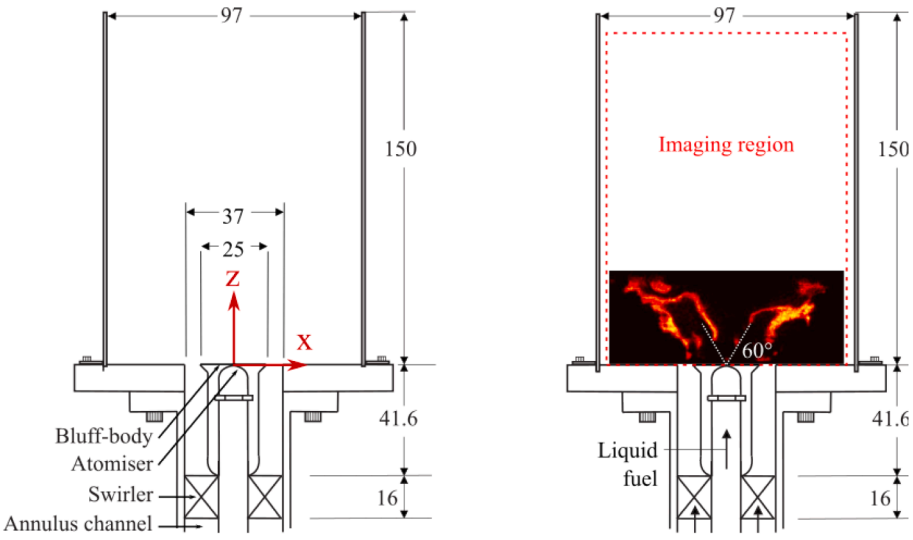

(a)

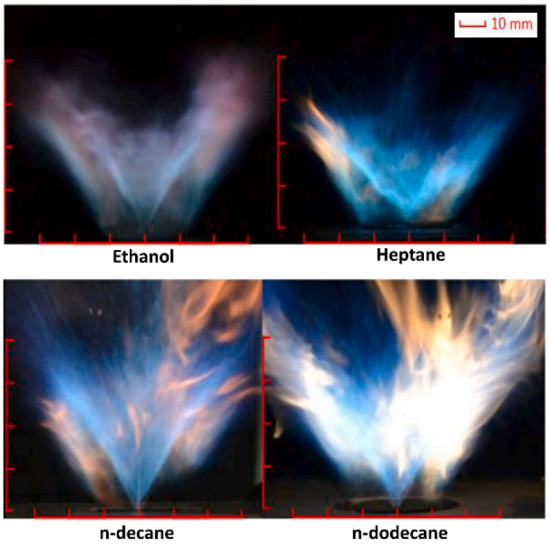

(b)

Fig. 2-1. (a) The Cambridge swirl-stabilised burner: (left) the geometry and (right) the imaging region where combustion takes place forming the 'M' shape flame, (b) is an example of the four different stable flames structure imagining generated using ethanol, heptane, *n*-decane and *n*-dodecane Sidey et al. [138] and Yuan [155].

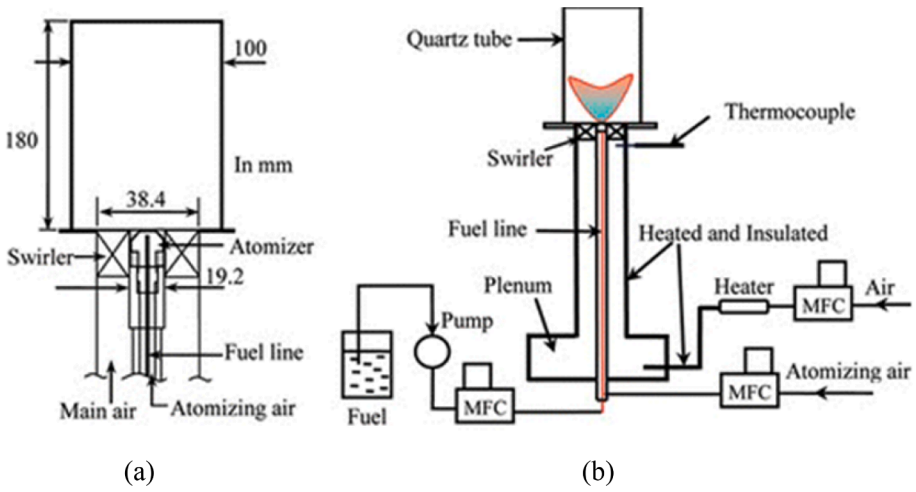

Fig. 2-2. (a) Swirl burner geometry; (b) Flow delivery system Chong and Hochgreb [20].

This non-exhaustive review covers, based on the criteria above, the laboratory scale burners developed for the purpose of supporting modelling development, over the last 30 years. However, due to the relevance and possibility of use in modelling validation, we have presented some laboratory-scale burners which did not meet these criteria but have justified their inclusion in section Summary of historical burners.

Types of burners

The relevance of laboratory scale burners

Experimental investigation of spray combustion processes involves the use of sophisticated and usually expensive optical diagnostic techniques that allow for the measurement of the gas-phase velocity and its fluctuating component, as well as droplets size distribution using, for instance, Phase Doppler Anemometry (PDA) techniques. Flame heat release, mixture fraction and flame topology can be assessed using spatially and temporally resolved Laser-Induced Fluorescence (LIF) and Planar Laser-Induced Fluorescence (PLIF) techniques measuring *OH* emission and chemiluminescence measurements of intermediate species such as *CH*, *CN* and *CO* amongst others; while soot and particulates have been measured mostly using Laser-Induced Incandescence (LII) [90], Vander Wal and Weiland [147] and Cheng et al. [18]. Experimental investigations using advanced and coupled optical diagnostics techniques play a crucial role in developing and understanding combustion sub-models (e.g., atomisation, evaporation, and turbulence-chemistry interactions).

Experimental databases for CFD validation are usually generated from small scale laboratory burners. Laboratory burners are designed with simpler and compact geometries (cylindrical or rectangular); the combustor section can be un-confined or confined (equipped with transparent walls usually made of quartz for full laser optical diagnostics and data acquisition) and either swirling or non-swirling [72] and Al-Abdeli and Masri [6]. Aeronautical gas-turbine burners are of the confined type and highly-swirling. The implications of confining the swirling flow are an increase in the velocity fluctuation field, enhancement of vortex breakdown and appearance of corner and wall vortexes; moreover, the flow Turbulent Kinetic Energy (TKE) in confined burners is almost double that of unconfined cases hence influencing the overall combustion dynamics [66]. Therefore, for the studies of aeronautical combustion, swirling and confined burners are more relevant than un-confined non-swirling burners because swirl can replicate flow recirculation, high anisotropy and instabilities that favour mixing sustaining chemical reactions.

Experimental databases from laboratory scale burners are used by CFD modellers in the development, modelling and validation of CFD codes, hence improving their accuracy. Therefore, by using high-fidelity CFD modelling subjected to extensive validation against data from laboratory scale burners, gas-turbine engine manufacturers can reduce the costs of the entire engine development life cycle [46]. In large scale gas-turbine engines, there is a prohibitive cost related to the manufacturing and assembly of the complex combustor components and testing and maintainability. Apart from the hardware cost, using laboratory-scale burners reduces the cost of CFD development as small geometries are more tractable to mesh and or require less mesh elements, thus, reducing the effective computational cost. Since computational time is saved, it gives room for the use of more sophisticated time-dependent three-dimensional turbulence models (Unsteady Reynolds-Averaged Navier-Stokes/Reynolds-Stress-Modelling (URANS/RSM) turbulence closure, Large Eddy Simulation (LES) and Direct Numerical Simulation (DNS)) that help in elucidating the intricate problems of the turbulence-chemistry interactions and the unsteady nature of finite-rate chemical kinetics in flame ignition, blow-off and pollutant formation [40].

Nonetheless, the scaling down process of an actual gas turbine combustor to a laboratory burner type is typically a complex problem. There are important non-dimensional parameters used in the design of laboratory burners in order to make them representative of large-scale gas-turbine engines [114] and Luo et al. [73]. Ideally, laboratory-scale burners have to be designed to function under similar operational conditions as in actual gas-turbine engines; for instance, the Swirl and Reynolds numbers and the Stokes and Weber numbers have to be akin to actual engine conditions. In addition, operational parameters such as the equivalence ratio, injection pressure and air inlet velocity must be in the same order of magnitude usually found in actual engines. Furthermore, flow recirculation and instabilities can be replicated by means of a confined swirl device, thus, making laboratory swirl burners representative of actual gas-turbine engines.

Confined burners

The Cambidge swirl-stabilised burner

The Cambridge swirl spray burner is an enclosed bluff-body experimental setup that displays vortex breakdown in the central recirculation zone. This setup focuses on the studies of highly swirling two-phase turbulent spray combustion using several operating liquid fuels from heavy carbon *n*-dodecane and *n*-decane to high volatile ethanol and heptane [16], Cavaliere et al. [17] and Yuan [155]. The burner aims to aid the understanding of the role of different fuels and intake velocities on ignition, global and local flame extinction of flames approaching

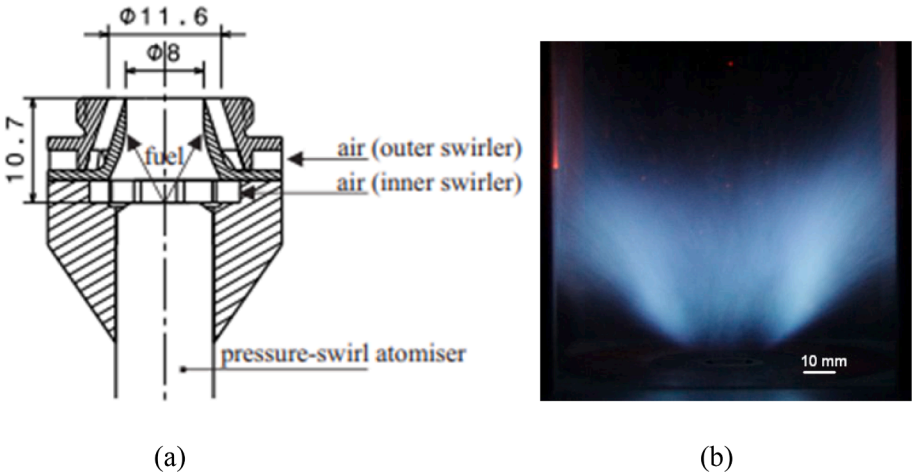

Fig. 2-3. (a) DLR burner nozzle detailed and (b) is a typical flame photograph burning Jet-A1 obtained from the experiment of Grohmann et al. [42,43].

blow-off; such phenomena are relevant for the understanding of the use of biofuels and flights under high altitudes, which directly impact the efficiency and operation of modern gas turbines [16], Yuan [155], Giusti et al. [38] and Giusti and Mastorakos [39].

The experimental setup is illustrated in Fig. 2-1. The combustor cross-sectional area is 95 × 95 mm^2 with a streamwise length of 150 mm. There is a geometric static six-vane swirl device that generates a strong clockwise swirl motion (when visualised at the nozzle from the combustion region) with a geometric swirl number (S_N) of 1.23 computed according to Beér and Chigier [7]. The air is injected through the annulus channel at ambient conditions (1 atm, 288 K) with the flow rate in the range of Q_{inl} = 500–990 SLPM (standard litre per minute) and bulk velocity of U_b = 14.3–28.2 m/s. A conical bluff-body with a diameter of D_b = 25 mm is concentrically fitted with the annulus channel. The flow is fully turbulent with a Reynolds number of 23 000; the recirculation flow and vortexes generated by the swirl motion can mimic the flow encountered in a gas-turbine.

The device uses a liquid-fuel hollow cone pressure-atomizer (Lechler 212 series) centrally located on the top of the bluff-body with a spray angle of 60° set up in a highly confined environment by a square of quartz that allows for non-intrusive optical access of the flame. The liquid mass flow is digitally monitored by a flow controller that measures with an uncertainty of ±0.02 g/s. Ignition of the flammable mixture is performed using laser sparks deposition and follows a similar approach developed in Letty et al. [70]. For stable ethanol fuelled cases, the burner achieved a thermal power output of 8 kW [115].

The Cambridge biodiesel swirl burner

The Cambridge swirl combustor geometry is of the confined type and is constructed using stainless steel; the walls are formed of quartz, as displayed in Fig. 2-2 [20]. It is made up of a swirl device formed of eight straight vanes at an angle of 45° that generates strong geometrical swirl intensity high enough (S_N = 0.78) to generate a central recirculation zone. This swirler surrounds a central tube which, in turn, leads to a plain-jet air-blast atomiser. The function of the central tube is to transport the fuel and atomising air to the atomiser, where atomisation takes place, and a liquid spray is injected. The liquid spray interacts with an envelope of coaxial swirling airflow in the combustor body. The fuel flow rate is controlled using Bronkhorst Coriolis mass flow controllers (M13 mini-CORI-FLOW) with an accuracy of ± 0.4 %, whereas the main air and atomising airflow rates are controlled using Bronkhorst thermal mass flow controllers (MFC) with an accuracy of 1 %. Additionally, two air heaters are used to heat the main airflow and the burner's plenum. The combustor also accommodates insulated materials around the body to reduce heat loss. The system enables the main air to be pre-heated to a temperature of 350 °C. To achieve a complete temperature control loop, a thermocouple is placed 10 mm upstream the swirler and provides feedback to the air heaters.

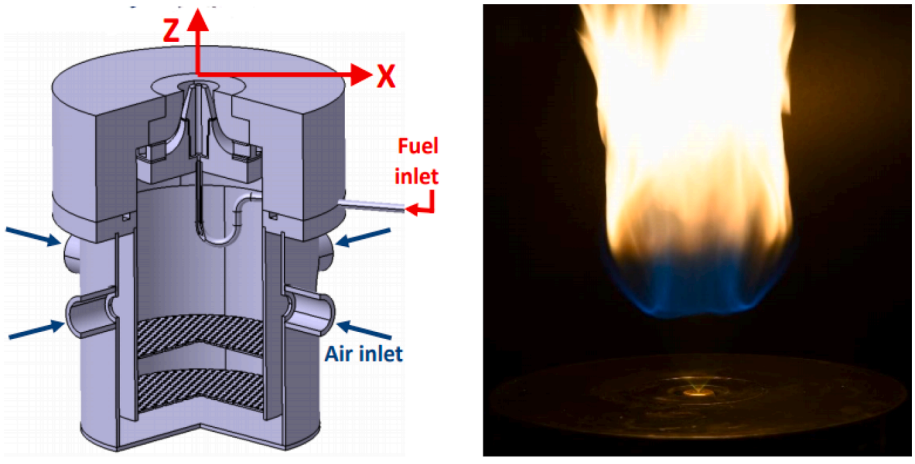

Fig. 2-4. CORIA burner (a) the injection system with fuel and air inlets and (b) stable jet spray flame topology Verdier et al. [148] and Renou et al. [122].

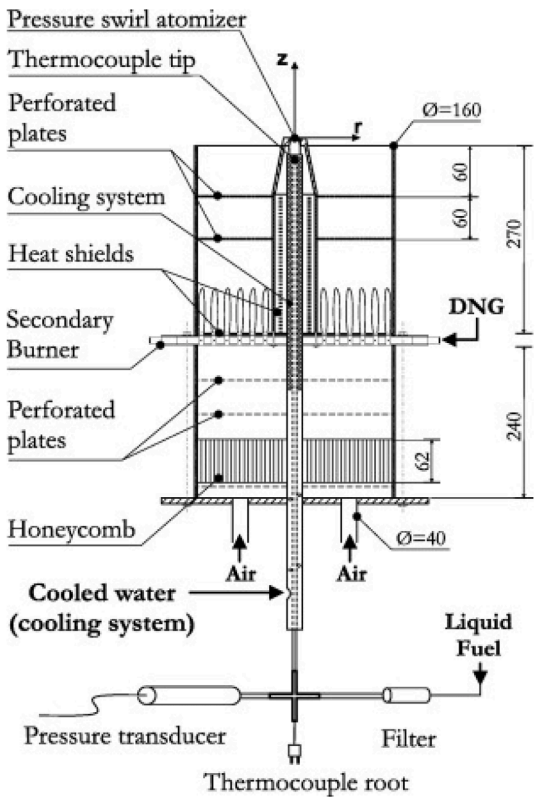

Fig. 2-5. DHSC setup Rodrigues et al. [126,127]. All dimensions in mm.

This burner has been used for studies of alternative fuels such as palm methyl ester (PME), which is considered as a promising biodiesel for application in gas turbines and furnaces [20].

The German aerospace centre (DLR) burner

The DLR developed burner is equipped with a complex nozzle (air-blast atomiser) which enables the formation of a hollow cone spray within a turbulent swirling flow field. The nozzle achieves this with the use of two swirling air inlets and a pressure-swirl atomiser, as illustrated in Fig. 2-3 (a); a typical compact swirl flame burning Jet-A1 is illustrated in Fig. 2-3 (b). The inner and the outer swirlers individually generate co-axial, co-rotating swirl flows, and a thin annular ring separates these two flows. The swirl number is strong for both cases at $S_N = 1.17$ and 1.22, respectively. The fuel is sprayed from the pressure-swirl atomiser at the inner side of this ring. The liquid film formed in this region is transported to the exit of the nozzle, where further atomisation takes place. The ability to capture the atomisation of liquid fuel and a swirling flow field in a confined combustor allows the DLR burner to obtain combustion characteristics close to real aero-engine characteristics [42,43]. The combustor pressure is 1 atm, and different mass flow rates in the range of 2.2–12.9 g/s are possible. The flow is fully turbulent with a Reynolds number of 25 000, and the burner operates with a global equivalence ratio of 0.8 and generates a thermal power output of 10 kW.

Unconfined burners

The CORIA jet spray flame burner

Fig. 2-4 (a) illustrates the jet spray flame burner geometry developed at the Complexe de Recherche Interprofessionnel en Aérothermochimie (CORIA). Fig. 2-4 (b) is a photograph of the *n*-heptane burning jet spray flame. This burner [48], named here as CORIA burner, uses a simplex fuel injector produced by Danfoss, which allows a mass fuel rate of 1.35 kg/h sprayed using an 80° hollow cone. The air inlet is non-swirling, and the flame occurs in an unconfined space under atmospheric conditions (T = 298 K and P = 1 atm); thus, the typical mechanism of flame stabilisation by swirl is not reproduced, and the flame stabilises with a high lift-off height with long, wide, and wrinkled flame branches. Both air and fuel flow rate are reported and measured by a thermal and Coriolis flow meters, respectively; the reported bulk velocity is 19.9 m/s. Detailed information on the injector geometry dimension, air velocity boundary conditions (mean and rms of axial and radial velocities) and fuel droplet height of atomisation, velocities and sphericity and their respective uncertainties is available in Fiorina and Van [34] or upon request as informed in Renou et al. [122].

The Delft Spray-In-Hot-Coflow (DSHC) spray burner

The DSHC burner generates turbulent spray combustion of ethanol under Moderate or Intense-Low Oxygen Dilution (MILD) conditions (flameless combustion) in order to provide a database for CFD model development and validation by measuring liquid break-up properties, flame temperature and lift-off behaviour in hot-diluted coflow [125] and Rodrigues et al. [126,127]. The experimental setup illustrated in Fig. 2-5 is an unconfined and non-swirling burner. The total height is 510 mm, and the outer diameter is 160 mm. The spray flame occurs in the unconfined region above the atomiser exit plane, and it is surrounded by both the hot-coflow and laboratory surrounding air. In order to prevent premature evaporation of the liquid ethanol fuel, the burner is equipped with a central water-cooling system and heat shields. Honeycomb and perforate plates are assembled, assuring that the secondary burner is fed

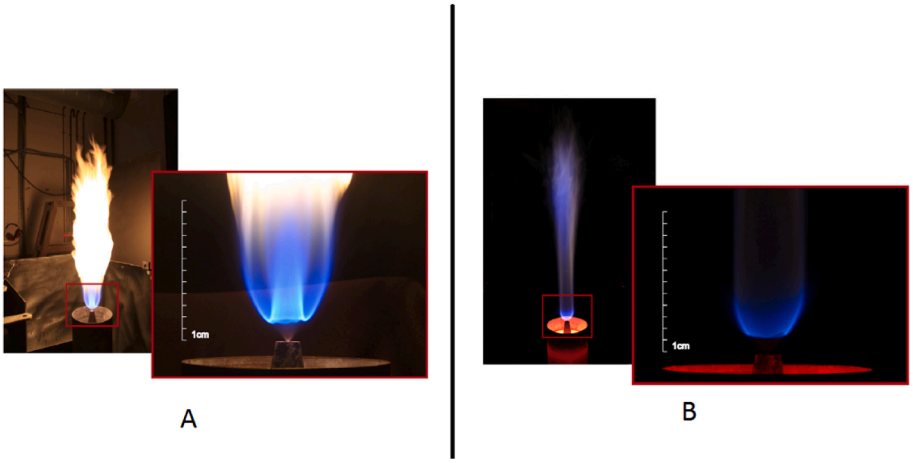

Fig. 2-6. a) shows a visual appearance of an ethanol turbulent spray flame with air as co-flow, whereas (b) shows a MILD piloted flame (with hot-diluted air), evidencing the changes in flame structure and the appearance of light blue-colour due to the low-temperature gradients Rodrigues et al. [126,127].

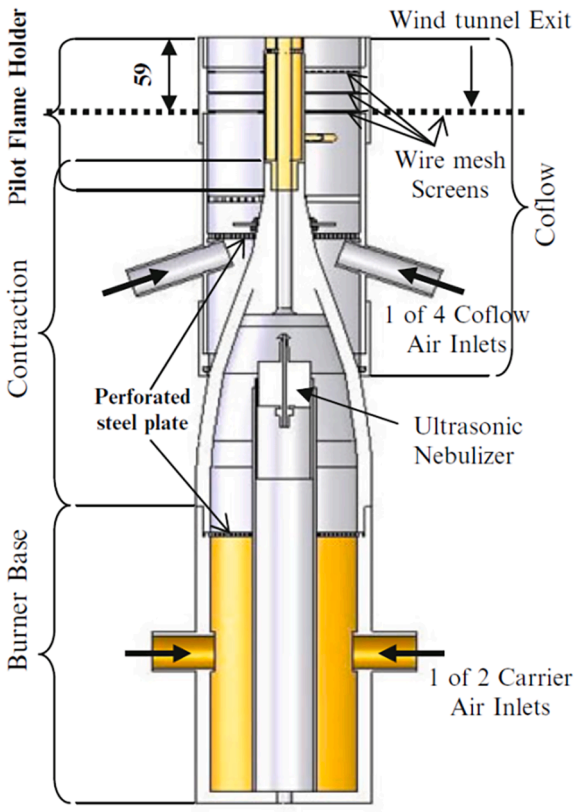

Fig. 2-7. Experimental apparatus depicting the main three geometrical parts from the bottom with the burner base, the contraction area with the ultrasonic nebuliser and the coflow ducts and the top part of the pilot flame holder Masri and Gounder [85].

with a homogenous and isotropic turbulence air. The injector used is a commercial pressure-swirl atomizer with a 60° solid cone. A secondary burner (known as pilot flame) fed with Dutch Natural Gas (DNG) fuel is placed inside the main burner, and it surrounds the spray flame (Fig. 2-6 (a) and (b)), serving as a forced stabiliser.

The Sydney spray burner

The piloted Sydney spray burner was developed in the studies of Masri and Gounder [85] and Gounder et al. [41]. A schematic of this piloted burner is shown in Fig. 2-7. The burner is constructed in four main sections with a total height of 595 mm. The carrier air-inlet is injected from the burner base, the contraction zone with four co-flow inlets accommodates the ultrasonic nebuliser (assembled inside the contraction central jet), and at the top is the pilot flame holder. The burner is non-swirling and unconfined; perforate annular plates are placed after the carrier air and after the co-flow air inlets (velocity at the exit is 4.5 m/s with low turbulence intensity); the spray flame is generated at atmospheric conditions. The whole burner is assembled in a vertical wind tunnel that provides the co-flow air streams. This burner features a piloted flame that is generated by burning a stoichiometric mixture of air-hydrogen-acetylene used to stabilise the central jet flame (pilot stream unburnt bulk velocity is 1.5 m/s).

Summary of historical burners

Of possible interest to the readers are historical burners pre-dating those in the present study. These burners (Tables 2-1 and 2-2) have essential datasets that are potentially relevant for the validation of droplets evaporation and spray combustion under stable conditions. There are 9 burners in total, and these are classified into Table 2-1 for alcohols and Table 2-2 for fossil fuels.

Experimental studies

Confined burners

The Cambridge Swirl-Stabilised burner

The main goal of the experimental study conducted by Yuan [155] was to generate boundary conditions and flame structure measurements database of recirculating spray flames for better validation and development of CFD codes at close to blow-off conditions. Combustion experiments were performed using high volatile (ethanol and *n*-heptane) and low volatility (*n*-decane and *n*-dodecane) fuels. The flame database was generated focusing on flames at conditions close to lean stability limits (approaching blow-off). A set of new measurements, data analysis and correlation techniques were developed to evaluate heat release rate, hydroxyl (*OH*) and formaldehyde (CH_2O) formation at the inner recirculation zone and along the outer shear layer edge. The low volatile flames were usually longer, straighter, and more anchored compared to high volatility flames. A first attempt at measuring the local equivalence ratio was successfully performed and with results with an error less than 20 %. At intense blow-off conditions, the flame starts quenching at the inner reaction zone of the central recirculation zone, and the flame is more attached to the bluff-body.

The evaluation of non-reacting (cold flow) mean and rms of the velocity fluctuations (axial, radial and swirl) fields were measured using one dimensional (1-D) Laser Doppler Anemometry (LDA). A total of 200 000 data samples were recorded from all the measurement locations with a statistical uncertainty of 1 %–3%. The bulk velocity is measured with an uncertainty of 3 % Cavaliere [16]. There are 9 axial measurements stations up to the outlet boundary; the first and nearest sampling station is at y = 8 mm. Therefore, the implementation of the inflow boundary condition cannot be transposed from the first location to the inlet plane at y = 0 mm; hence modellers need to either simulate the entire burner including the swirl (through the vane approach) device or estimate the velocity profile by means of trial-and-error approach; inflow turbulence data for both LES and Reynolds-Averaged Navier-Stokes (RANS) initialization cannot be inferred nor extrapolated. Cold flow non-reacting results are composed of mean and rms of the three velocity components (axial, radial and tangential) and turbulent kinetic energy, as reported in Cavaliere [16].

The application of Laser-Induced Breakdown Spectroscopy (LIBS) for

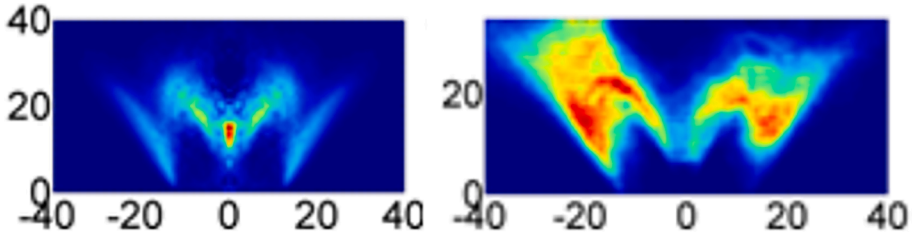

Fig. 3-1. Ethanol 'E1S1' flame. (a) mean *OH*-PLIF and (b) mean *OH** chemiluminescence (after inverse Abel transform), indicating the 'M' shape heat release rate (*HRR*) areas. Flame 'E1S1' is approaching blow-off. Adapted from Yuan [155].

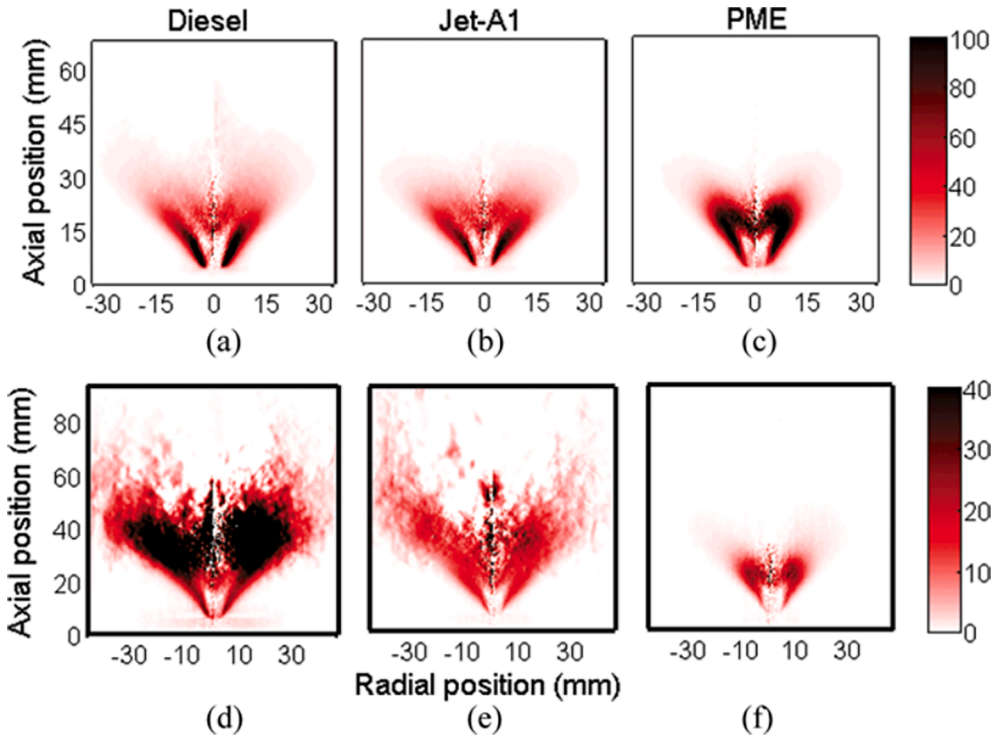

Fig. 3-2. Images (a), (b) and (c) represent Abel transformed CH* chemiluminescence while (d), (e) and (f) use a broadband long-pass filtered signals that are used to analyse soot emissions Chong and Hochgreb et al. [20].

the measurements of the local time-averaged mixture fraction of heptane [155] and ethanol was reported in Giusti et al. [38], covering a wide range of mixture fractions; the mixture fraction data from the LIBS measurements were plotted at four different heights from the bluff-body. The reported variance for a single shot-to-shot LIBS measurement was around 15–20 %, and it was speculated that the presence of liquid droplets in the background, fluctuations of the laser energy and collection delay time might have interfered with the plasma emission spectra measurements [155]. The results for ethanol indicated a predominance of fuel-rich mixture up to location y = 20 mm (flame centre), while for locations further downstream, far away from the injector, the mixture was homogenous and lean-fuel conditions appeared.

Fig. 3-1 shows the imaging results for the ethanol flame known as case 'E1S1′ ('E' stands for Ethanol, 'S' stands for stable). This flame has a bulk velocity of 17.1 m/s and a fuel injection velocity of 10.68 m/s; this bulk velocity represents 79.2 % of the blow-off velocity, which means this flame is approaching blow-off. The overall equivalence ratio is 0.23. The mean OH-PLIF is used to mark the flame structure, while OH^* chemiluminescence (after the Abel transform) marks the regions of heat release rate (HRR) obtained from the joint 5 kHz PLIF measurements between OH-PLIF and CH_2O radicals. Yuan [155] found that the product $CH_2O \times OH$ is suitable for marking the spatial distribution of HRR for both non-premixed and premixed flames; from these results, semi-quantitative analyses such as the maximum flame height and the thickness of the reaction zone can be inferred. Related results as presented in Yuan [155] were also obtained for heptane, *n*-decane and *n*-dodecane. Complementary studies of the spray evaporation process and flame structure analyses using measurements of the $CH_2O \times OH$ were performed in Kariuki and Mastorakos [58].

The Cambridge biodiesel swirl burner

The characterisation of the axial and radial velocity profiles for the non-reacting flow are measured using 2D-PIV in Chong and Hochgreb [19]. For the reacting flow conditions, PDA was extensively used for the measurements of the droplets axial velocity components and SMD. Measurements near the dense spray exit region were not carried out due to limitations in the PDA measurements. Measurements were taken from the burner outlet at three downstream axial locations starting at 10, 15 and 20 mm. In this area, the spray is no longer influenced by the dense cloud of liquid droplets, and a polydisperse behaviour was observed; thus, this allowed for the measurements of droplets velocity and size with a good statistical uncertainty of 2–5 %. For the three fuels tested, the droplets velocity is almost the same at locations 10 and 15 mm, while an increase for PME is observed at 20 mm, which was associated with the higher density and surface tension values of PME; the same trend appears in the SMD values. The influence of the recirculation zone flow is reflected in the lower droplet velocity at the centre.

The flame structure is captured using data from the CH* chemiluminescence measurements (as revealed in Fig. 3-2 (a) to (f)). This allows for direct comparison between different fuels using the same equivalence ratio; the PME flame, for instance, has some distinct features, such as a more intense heat release in the central flame and a shorter height. From this data, the flame length and width can be deduced [19].

Furthermore, emissions measurements of NO_x, CO and soot were carried out at the combustor outlet using a typical commercial gas analyser. It is worth mentioning that a slight reduction in NO and NO_2 for the case, using PME is achieved compared with its fossil fuel counterparts, as explained, this is mostly due to the oxygen present in the PME, which may suppress CH production. Overall, PME showed no sign of soot, with a more "bluish" premixed behaviour, or it can be seen as insignificant compared to Jet-A1 and Diesel, which tend to produce more soot with high luminosity near the burner outlet.

The DLR burner

The experimental study conducted by [42,43] compared the combustion characteristics of liquid single-component hydrocarbons (*n*-hexane, *n*-dodecane and isooctane) and Kerosene Jet A-1, using the DLR burner. This study presents flow field measurements, CH* chemiluminescence, Mie scattering of fuel droplets, and lean blowout

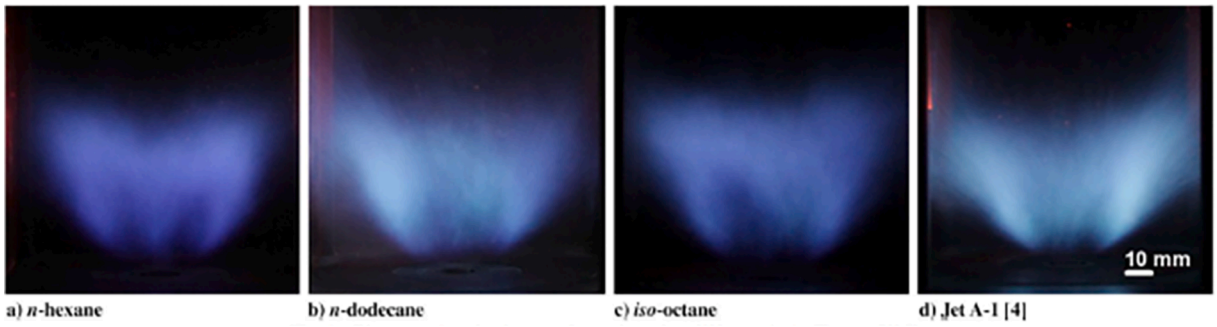

Fig. 3-3. Typical images of the swirl flame burning on *n*-hexane, *n*-dodecane, isooctane and Jet A-1 Grohmann et al. [43].

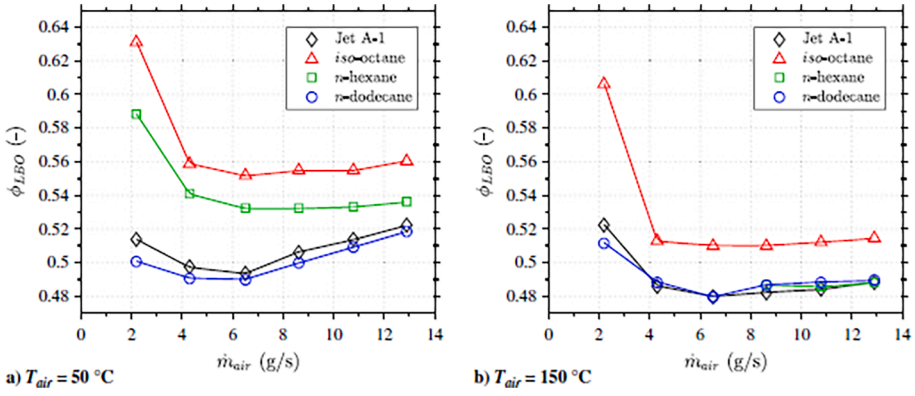

Fig. 3-4. Lean blowout results of the selected fuels at two air preheat temperatures Grohmann et al. [43].

measurements for *n*-hexane and *n*-dodecane. Kerosene Jet A-1 is used for comparison. It was reported that the typical combustor inlet temperatures for lean blowout start at 125 °C; however, 50 °C was chosen as this was below the boiling point of all tested fuels. This prevented the vaporisation of the fluid in the feed line. The wall temperature, which varies in the range from 450 to 1150 °C, was measured.

Stereo PIV was performed at three regions of choice in the study undertaken by [42,43]. A high spatial resolution was used to capture the measurements at the nozzle exit region ($y = 0.4$ mm); therefore, average velocity fields (radial, axial and tangential profiles) were provided, and the central recirculation zone was identified for non-reacting flow with pure air and fuel load. On the contrary, a lower resolution was chosen for the remaining part of the combustion chamber with two staggered fields of view. The results obtained were then post-processed using a stereoscopic multi-pass PIV algorithm. As well as this, the lean blowout was detected visually, and the corresponding equivalence ratio was recorded. Additionally, the chemiluminescence signal of the electronically excited *CH* radical was measured for Jet A-1. The post-processing included the subtraction of background and white images as well as the averaging of 1000 single images. This allowed for a semi-quantitative characterisation of the flame structure in terms of its maximum height (50 mm), and the typical swirl M shape can be quantified as well as regions where the flame interacted with the walls.

The flames for the selected fuels at reference conditions are shown in Fig. 3-3. These reference flames have a global equivalence ratio of 0.8.

This study also graphically presents the lean blowout results of the selected fuels at the two preheat temperatures as replicated in Fig. 3-4. The influence of the air mass flow rate on the global equivalence ratio at which blowout occurs is vividly depicted. It can be inferred that the general trend of the curves is similar for all fuels: as the air mass flow rate decreases, the global equivalence ratio also decreases before increasing at very low air mass flow rates. As well as this, at 50 °C, isooctane has the highest global equivalence ratios, and *n*-dodecane has the lowest, closest to that of Jet A-1. *n*-hexane appears to show intermediate characteristics comparatively. This study reports that at higher airflow rates, atomisation and mixing is enhanced, but high strain rates limit flame stabilisation. Conversely, the strain rate decreases at lower airflow rates while residence time increases, but fuel atomisation degrades. Additionally, another inference from the results is that higher preheating ($T_{air} = 150$ °C) improves the lean blowout limits for high air mass flow rates.

This study also presents conditional liquid loading profiles, and radial Sauter mean diameter profiles for reference flames at two distances from the exit plane. In summary, this study demonstrated that differences in lean blowout characteristics for different fuels are likely due to differences in the physical and chemical properties of these individual fuels. The authors also suggested that the influence of flame-wall interactions should be explored by measuring flame positions at very lean conditions for the different fuels. Another suggestion is to investigate the lean blowout performance of the four fuels at higher pressures and temperatures.

Unconfined burners

The Delft spray burner

Detailed measurements of ethanol jet liquid breakup and spray flames in both non-swirling air coflow and hot-diluted coflow (MILD combustion at T = 1200 K, generated with a burner fuelled with Dutch Natural Gas (DNG) under lean conditions) were carried out using Coherent anti-Stokes Raman Spectroscopy (CARS), conventional LDA/PDA and high-speed visualisation cameras [125] and Rodrigues et al. [126,127]. The gas-phase temperature (including regions with high droplet density) was quantitatively measured using the CARS, which is a central contribution of this burner platform. This technique was also combined with a high-speed visualisation camera in order to address the dense spray phase and understand how the liquid jets break-up under different coflow conditions. Conventional LDA and PDA systems were applied at several axial locations (starting at z = 0 mm, the injector exit

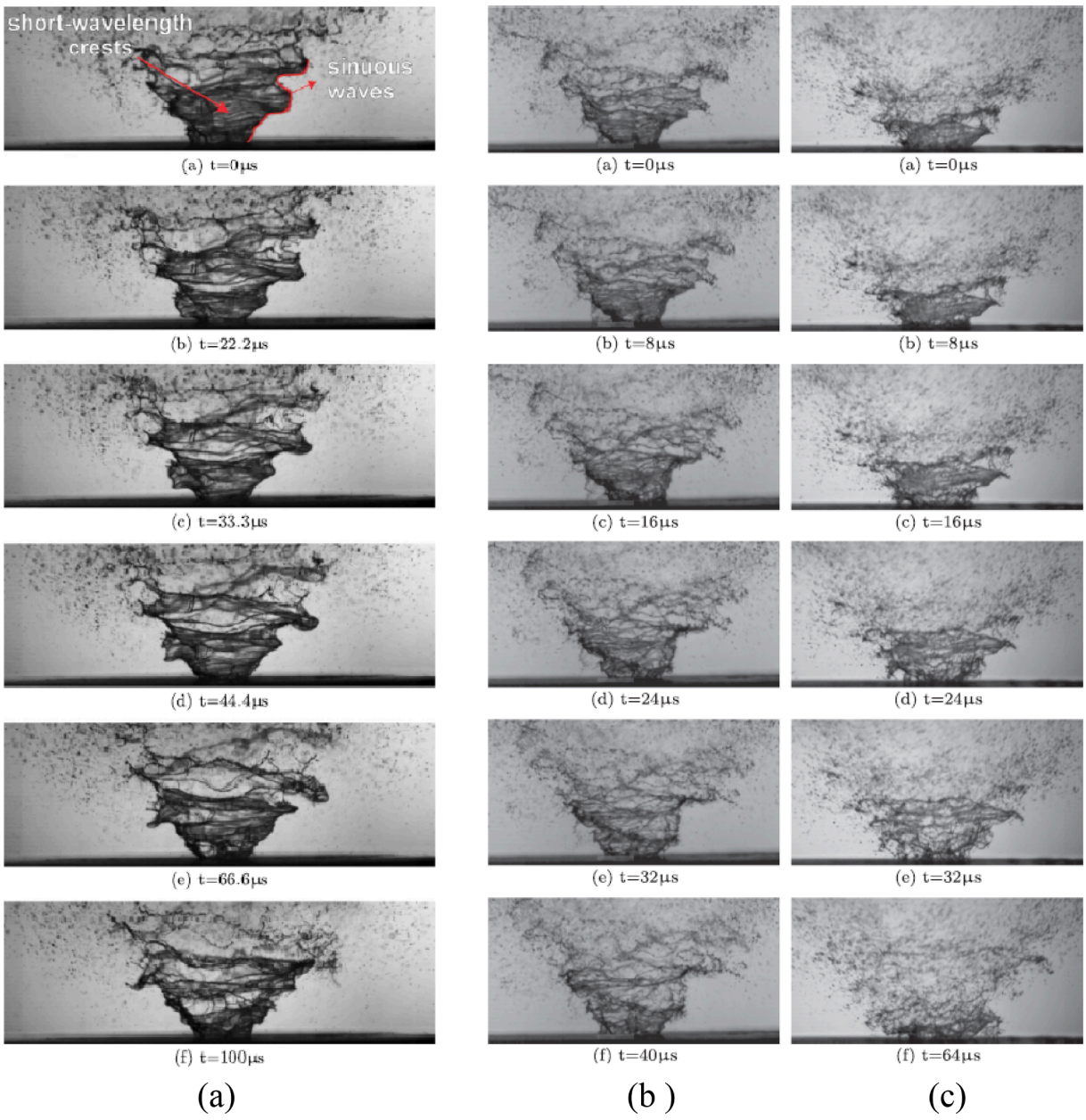

Fig. 3-5. (a) Non-reacting spray break up, (b) reacting spray breakup in air and (c) spray in hot-diluted co-flow. It is adapted from Rodrigues et al. [127].

plane) for the measurements of the gas-phase velocities statistics and droplets velocity and size statistics in the spray region. The overall error is up to 4 %; Axial and radial velocities profiles and their fluctuation components are recorded at location z = 0 mm, the data are presented as Favre-averaged quantities, and the estimated error is 2 %. The liquid fuel and air coflow flow rates, pressure and temperature, were measured using conventional Coriolis-flowmeters, pressure transducer and a type K thermocouple; the data is collected using a dedicated data collection system and the scalar values are tabulated. A flue gas analyser with an inaccuracy of 0.20 % is employed for the measurement of the oxygen volume fraction at the exit plan, and the profiles of the mean oxygen volume fraction at z = 0 mm are plotted for the flame with hot-diluted coflow.

Fig. 3-5 shows the high-speed images of the liquid breakup mechanism for the non-reacting case in air co-flow (a), reacting in the air (b), and reacting in hot diluted co-flow (c). Overall, the strong influence of the hot-diluted gases in the droplet atomisation speed-up the evaporation rate near the exit plane, causing faster fragmentation of the liquid sheet from the main liquid conical sheet at the exit plane. The typical sinuous waves disturbance in the non-reacting and reacting air coflow cases was not observed in the hot-diluted coflow case. It is believed that this phenomenon is related to a distinct turbulence modulation (due to vaporization) near the atomiser region, and the experimental database correlated plots of the gas-phase velocity and temperature with droplet size distribution in order to shed light on turbulence modulation phenomenology.

The jet spray flame

Fig. 3-6 (a) and (b) illustrate the region of measurements and the spatial distribution of the extensive optical diagnostics apparatuses (PLIF, PIV and Shadowgraph) used in the experiments of [122]. The data generated by these experiments allowed the assessment of several atomisation and combustion processes. For instance, the droplets sphericity is measured using shadowgraphy, which can cover an area very close to the spray exiting jet, thus allowing the measurement of fuel droplet, ligaments and conical sheet images. High-speed *OH*-PLIF is

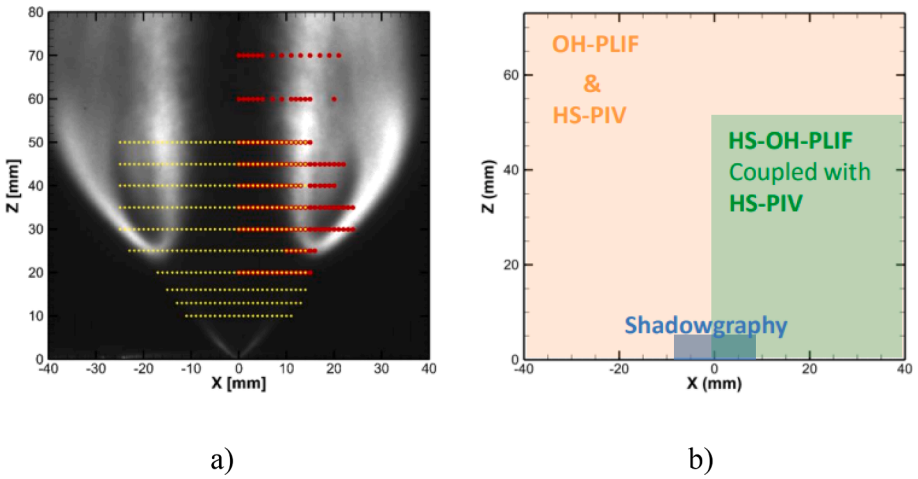

Fig. 3-6. (a) Flame measurement points and (b) the spatial area covered by the optical apparatus Renou et al. [135].

applied for the assessment of flame extinction and re-ignition phenomena. The authors reported that during the experiments, a large quantity of data was generated for the *OH*-PLIF, which lead to data storage and sharing issues. Also, High-Speed PIV was used for the characterization of the air velocity and turbulence flame interactions which is a straightforward way to determine the flame position coupled with the velocity field; these results are obtained from the reports of Fiorina and Van [34] and Renou et al. [122].

With regards to the fuel droplet temperature measurement, the studies of Verdier et al. [148] made use of the Continuous Global Rainbow Refractometry Technique (C-GRT) and Instantaneous-GRT, which allowed not only droplet temporal average temperature measurements but also in combination with *OH*-PLIF the measurement of the fuel droplet temperature conditioned by the distance to the flame front in various regions of the flame. Furthermore, the authors presented some new insights toward understanding the physics of the temperature of the droplets near the flame front and showed the strong influence that the history of the droplet motion has on the droplet temperature in different axial sections and its influence on the flame structure.

PDA was applied to measure the droplets and air velocity properties in Verdier et al. [148]. Both the mean axial gas velocity and droplets mean diameter/size distribution were obtained in the streamwise direction (Z) at distances of 5 mm-13 mm and 13 mm, respectively. Moreover, PDA was applied in combination with *OH*-PLIF to characterize the two-dimensional flame shape, for instance, to identify the two distinct reaction flame zones, namely an inner structure zone with small droplets and a high *OH* gradient, demonstrating that partially premixed combustion governs the reaction and an outer structure where there is a predominance of large droplets. One of the conclusions of this analysis is that there is an equilibrium of droplet evaporation between the two reaction zones.

The Sydney spray burner

The main findings and boundary conditions for both non-reacting and reacting cases of the piloted diluted spray burner studies are distributed through Masri and Gounder [85], Masri and Gounder [84] and Gounder et al. [41]. A total of 24 cases (8 non-reacting) are measured for both Acetone and Ethanol; different spray loadings and carrier velocities are investigated and the influence of these parameters on steady flame structure and blow-off are investigated using Laser-Induced Fluorescence imaging (LIF), Mie-scattering, (LDV) and PDA techniques. The droplets generated by the ultrasonic nebuliser have zero momentum and an SMD of 40 μm before being carried by the co-flow air.

The measured data for the carrier air mass flow rate and velocity, fuel flow rate, fuel vapour flow rate at the jet exit plane and fuel and air temperature are tabulated for each flame case. Droplet quantities (axial and radial velocities, diameter, number density and volume flux) and gas-phase velocity are recorded at seven different axial locations using the LDV/PDA system. Non-reacting measurements using Acetone spray were carried out for the validation of the dispersed phase starting at 3.15 mm downstream of the burner's exit plane. Graphics of mean and rms fluctuations of the droplets axial velocity are presented for the reacting ethanol and acetone cases at 5 different locations, starting at 3.15 mm downstream of the burner exit plane; the results are presented

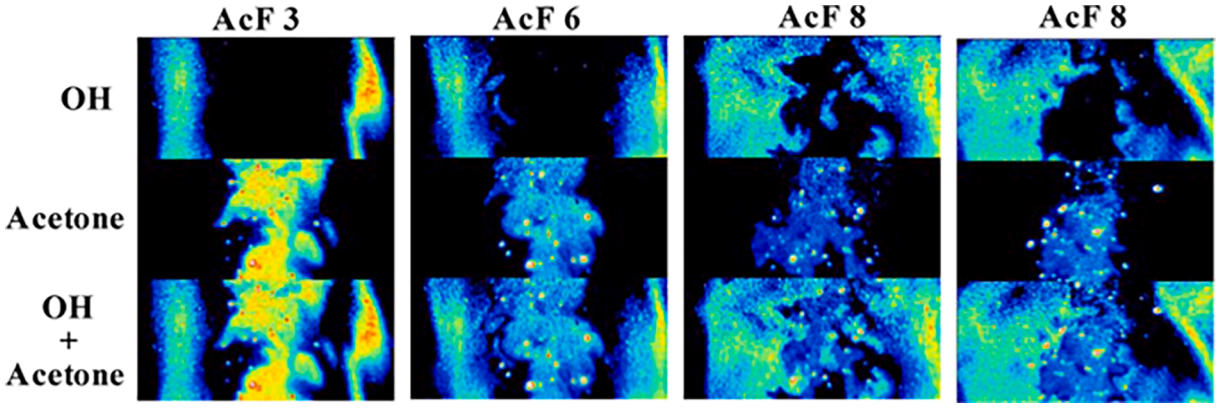

Fig. 3-7. Typical simultaneous flame imagining for Acetone spray obtained with the joint LIF-*OH*-Ethanol; case AcF8 is approaching blow-off Masri and Gounder [85].

conditioned to droplet size distribution, and there are also droplet size distribution PDF plots.

Anomalies in the droplets rms of the velocity fluctuations measurements were reported [84] to be influenced by droplets shedding from the wall liquid film; hence this complex phenomenon should be carefully considered while establishing CFD boundary conditions and validation of results. Typical errors involved in liquid and carrier air flowmeters are 5 % and 1 %, respectively. The challenging liquid volume flowrate measurement at the burner's exit plane presented an average discrepancy of 15 %; the maximum estimated errors with the LDV technique are 6 % for mean axial velocity and 15 % for its rms fluctuations.

Reacting cases were investigated using a joint measurement of LIF-*OH*, LIF-*OH*-Acetone and Mie-scattering and semi-quantitative data generated from these. These provided semi-quantitative information on flame structure and droplet location as well as indicating zones of hot spots and high evaporation. The gas-phase temperature was measured using an R-type thermocouple, and plots of the radial mean excess temperature profiles are shown in Masri and Gounder [85], accompanied by comparative results between flames. Overall, the differences in temperature in various sections of the flame suggested a competing phenomenon between non-premixed and premixed regimes; corrections in the measurements due to radiation and thermocouple quenching are not accounted for; thus, the uncertainties in temperature measurements could not be estimated.

Fig. 3-7 shows a typical simultaneous Acetone flame structure which is captured using joint LIF-*OH*-Acetone considering 4 different cases. Similar measurements and analyses are presented for the Ethanol flame. These qualitative measurements data are used along with temperature measurements to shed light on how different fuel loading and carrier velocity values influence the flame combustion modes (non-premixed and premixed) across different spatial locations. Flames AcF3 and AcF6 (low velocity) in Fig. 3-7 show a thin region of *OH* that is separated from the Acetone vapour-liquid fuel, thus behaving in a non-premixed mode. On the other hand, the two consecutive snapshots of flame AcF8 (high velocity) in Fig. 3-7 reveal a more premixed mode with large regions of *OH* intercalating with the Acetone vapour-liquid fuel; these distinct features can also be examined in conjunction with droplet measurement and temperature data in analysing the flame blow-off physics.

Computational modelling

The main numerical methodologies applied in the simulation of the burners presented in sections Confined burners and Unconfined burners are now presented and discussed; this non-exhaustive review of numerical modelling has covered a period of 26 years (1996 to 2022). Spray combustion simulations have been predominately carried out using finite volume steady-state isotropic RANS and, more recently LES turbulence modelling; there is a preference for using Eulerian-Lagrangian approaches coupled in a two-way manner to account for mass, energy and momentum transfer between the phases. Combustion modelling has been predominantly computed using tabulated chemistry models, especially the flamelet/progress variable, the Flamelet Generated Manifold (FGM) and Conditional Momentum Closure (CMC) approaches.

Overview of CFD combustion modelling

The development of CFD codes for spray flames simulations is a complex task because it requires the coupling of several different techniques to represent the gas-phase motions, the modelling of the droplet breakup, heat transfer and evaporation, as well as the turbulent interaction coupling between the gas and liquid phases Kuo [69]. The combustion modelling has to be coupled to represent the burning of individual and groups of droplets and usually requires detailed chemical mechanisms with thousands of reactions and hundreds of species. Spray combustion usually involves swirling motions under high Reynolds number values and is hence inherently turbulent and multiphase due to evaporation. Thus, an appropriate turbulence modelling that can represent the large scales where mixing occurs between the evaporated phase and the oxidizer is required. Turbulence modelling studies have been mostly carried out using RANS models using two-equation closure and simplified swirl boundary conditions. The combustion processes are modelled using the Eddy Dissipation models [32], Lewandowski et al. [71] and Ertesvåg [33]; the reduced chemistry Flamelet models Peters [107–110], Maas and Pope [82], Flamelet Generated Manifold [100], Oijen et al. [87,95–97,101–102] and Oijen and Goey [98–99] and the CMC model Klimenko [67], Giusti et al. [38] and Giusti and Mastorakos [39], amongst other modelling techniques. LES and models based on the Probability Density Function (PDF) [106] and Jones et al. [54] for turbulent spray flames have recently become more feasible for industrial applications due to the increases in computational power in the last two decades. Despite continuous improvements in computational power and combustion modelling, applying LES and DNS on real scale aeronautical combustors is still costly and intractable. Especially modelling the entire flame envelope (forced ignition, stabilised and extinction operations) and the majority of the combustion modelling still pertains to the academic setting with a focus on laboratory scale burners [103], Poinsot and Veynant [115], Jenny et al. [53] and Poinsot [114].

The application of DNS has been limited to canonical and theoretical flame problems with low to moderate Reynolds number, as in Réveillon and Vervisch [123], Domingo et al. [26], Luo et al. [73] and Pillai and Kurose [113]. In these studies, fundamental questions were addressed to support sub-grid (SGS) model development for LES and help in the elucidation of flame ignition and extinction issues. Exploratory studies have also helped in elucidating some aspects of the dual nature of spray flame that can manifest non-premixed and premixed combustion modes (partially premixed phenomenon) at distinct spatial locations. Furthermore, DNS data have been useful in improving the understanding of the turbulence-chemistry interaction (flame regime) in spray flames. However, limitations due to low Reynolds number and poor chemistry resolution (use of simplified and single global chemical kinetics) mitigates its potential in fully underpinning the physics of typical aeronautical engines where Reynolds number values are high, and the intermediate species (finite-rate chemistry) play a vital role in determining the combustion processes. Thus, the DNS potential can be undermined when capturing the ignition patterns, flame structure and heat release, burner power output, flame lift-off and pollutant emissions. Therefore, while it is true that DNS possesses the potential for solving the entire turbulent spectrum, its application in real gas-turbine geometries for spray reacting flow is still expensive and would require the use of Exascale computing as well as more efficient parallel platforms and algorithms [35]. However, the development of CFD codes validated with robust validation test datasets are needed to exploit rapidly advancing High Performance Computing hardware Slotnick et. al [137].

Confined burners

The Cambridge Swirl-Stabilised burner

The Cambridge swirl stabilised burner has been simulated using ethanol in Giusti et al. [38] and Giusti and Mastorakos [39], *n*-heptane in Tyliszczak et al. [140] and Paulhiac et al. [104] and *n*-dodecane in Mohaddes et al. [92]. Giusti et al. [38] carried out CFD simulations of the burner in section The Cambridge swirl-stabilised burner using the LES code PRECISE-UNS for gas-phase and spray. The CMC equations were solved by the author's in-house code coupled with tabulated chemistry by using density and temperature data. The swirl inflow condition was set using constant profiles of inlet velocities, and the swirl device was not included in the domain; the cold flow validations were carried out using the mean velocities profiles against experimental data, but the detailed assessment of the turbulent kinetic energy and turbulence structures within the Central Recirculation Zone (CRZ) was missing. The influence of the spray source terms was neglected on the

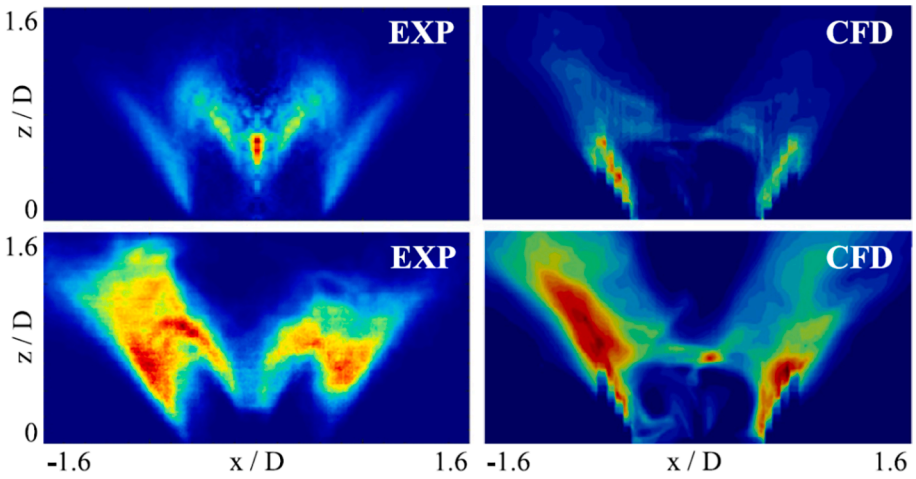

Fig. 4-1. Comparison between LES-CMC simulation against experimental data for flame 'E1S1′. Top row: indicates the experimental inverse Abel-transformed time-averaged *OH** (heat release rate (*HRR*); bottom row: mean of *OH*-PLIF indicating flame structure (EXP) and the mean *OH* mass fraction (CFD) Giusti et al. [38].

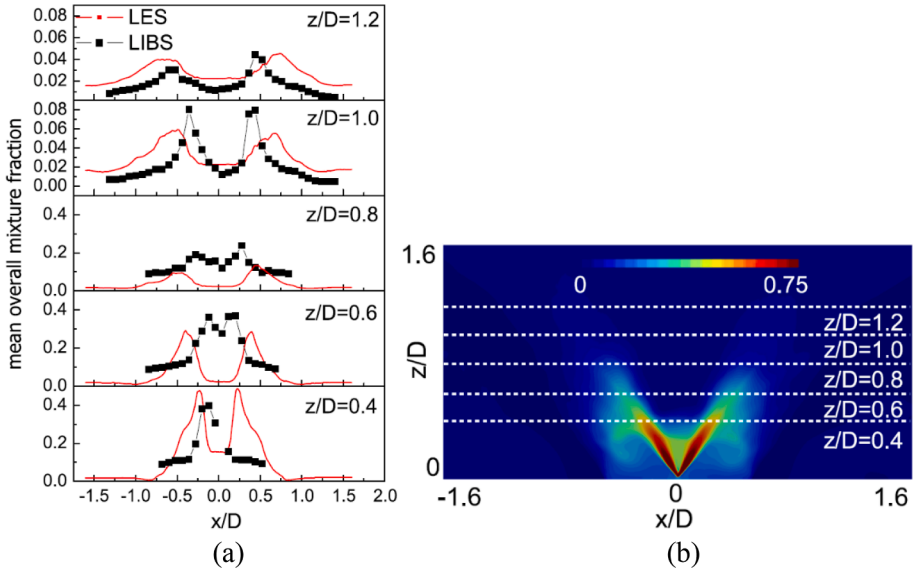

Fig. 4-2. (a) Mean overall mixture fraction, LIBS technique and (b) LES instantaneous snapshot of mixture fraction with the probe stations lines for flame 'E1S1′ Giusti et al. [38].

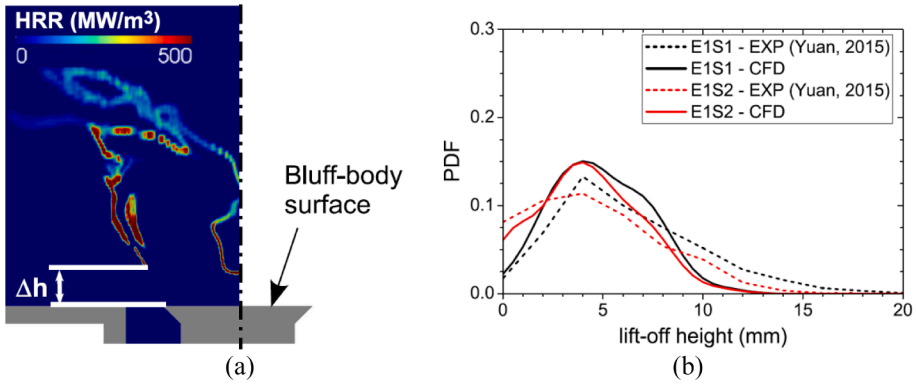

Fig. 4-3. (a) The flame lift-off height from the top of the bluff-body; (b) the statistics of the experimental and numerical lift-off for flames E1S1 and E1S2 approaching blow-off Yuan [155] and Giusti et al. [38].

combustion equations; the number of computational parcels used for the spray boundary condition and the spray velocity was not presented, and the convergence and stability criterion of the Lagrangian solver was not investigated. The chemistry-combustion table was generated using an unsteady zero dimensional (0D) CMC approach which is similar to the generation of FGM tables but without the inclusion of heat loss and gain; the numerical procedure to ignite the mixture was not investigated; a single step global chemistry mechanism for ethanol was applied.

The main results of using LES-CMC were compared against the experimental data for flame 'E1S1′ in terms of mean of flame HRR and mean of OH mass fraction spatial distribution (Fig. 4-1), the LIBS mixture fraction (Fig. 4-2) and the flame lift-off values (Fig. 4-3).

As observed in Fig. 4-1, the major semi-quantitative characteristics displayed by the ethanol flame were not well-captured. Three issues were observed; especially at the centre of the CRZ, the experimental HRR indicates a bright and intense 'V' shape located at the centre of the CRZ, this feature was not captured with the LES-CMC as evidenced by the absence of the *HRR* in this region; at this same location the mean *OH* mass fraction from the LES indicates a thin and long region (at the centre of CRZ) while the experimental mean *OH*-PLIF results indicate a complete and connected 'M' shape; overall, the LES *OH* mass fraction data is asymmetric and suggested that the flame extended up to the walls at location Z/D 1.6, and this was not observed in the experimental mean *OH*-PLIF data. According to Giusti et al. [38], this might be attributed to issues related to spray boundary conditions and inefficacy in defining the sub-grid for the LES spray due to the evaporation effects as well as due to uncertainties related to the spray cone angle and spray injection velocity which were challenging to match against the experimental data.

Overall, the LES-CMC results in Fig. 4-2 indicate a considerable mismatch (up to one order of magnitude) for the mixture fraction. This occurred especially at the centre of the CRZ at a location near the injector (z/D = 0.4 and 0.6) up to the flame centre (z/D = 0.8). There is a pronounced asymmetry for all locations evaluated, while the peaks of the mixture fraction were usually over predicted for locations near the bluff-body ($z/D = 0.4$) and under predicted from the downstream where the mixture becomes more uniform due to more intense mixing. According to Giusti et al. [38], this might be associated with issues with spray boundary conditions, chemistry modelling and LES sub-grid modelling in capturing the influence of evaporation in the mixture fraction; attention was called to the need for further developments to tackle these issues.

Fig. 4-3 shows the ability of the CMC model to capture the ethanol flame lift-off; the reported mean value was 6.25 mm [155]; the LES lift-off was underestimated with a peak value of the PDF around the lift-off height corresponding to 5 mm; the deviation is more pronounced for values of lift-off greater than 9 mm, while for values between 0 and 5 mm the values are comparable. According to Giusti et al. [38], this wide variability in the lift-off values is driven by the higher fluctuations in the turbulent field near the top of the bluff-body. According to Giusti et al. [38], one of the ways to improve the prediction of flame-lift-off would consist in applying detailed chemistry mechanisms and improving the mixture fraction equations to account for the effects of evaporation.

The computation of the constant scalar dissipation rate, which is a parameter that requires tuning, was carried out based on previous SANDIA flame studies, and the parametric results that lead to the definition of the constant value were extrapolated for the spray flames application [38]. A parametric analysis using different values for the constant value in the scale dissipation equation would be worth studying because the extinction phenomena are so sensitive to this parameter. Regarding the chemistry modelling, the authors opted for single one-step chemistry to reduce computational time; it was calibrated using data from the detailed chemistry. The calculated scalar dissipation for the one-step mechanism rate was 267 1/s, despite the claim that it is not too far from the 367 1/s obtained using detailed mechanisms. Comparative studies using both mechanisms with different scalar dissipation were not performed Giusti et al. [38].

Since the flame is sensitive to the boundary conditions as previously shown herein, one of the potential drawbacks for further scientific reproduction of this experiment is that the hollow injector does not behave as a perfect cone, and the authors have applied a stochastic method to reproduce this abnormality since positive axial velocity was found at the outlet. Therefore, it might require a significant trial-and-error approach to match the experimental data. However, they have not published this stochastic method which successfully overcame this issue, and only a short explanation was introduced; no further reference was mentioned. Another unexplored assumption was the extent of the accuracy of the first-order closure method for chemistry modelling Giusti et al. [38].

An interesting issue raised by the authors was the importance of accounting for the evaporation micro-mixing effects on the LES sub-grid scale mixture fraction variance. They pointed out that this parameter strongly influences the computation of the sub-grid scale scalar dissipation rate and the importance of not neglecting this term. However, the authors opted for using a simplified algebraic expression instead of those equations previously suggested by Pera et al. [105] and Reveillon and Vervisch (2000). This topic remains open and requires further studies.

Mohaddes et al. [92] simulated this same burner configuration with *n*-dodecane, and the combustion model included the effects of low-temperature chemistry using the commercial compressible LES code CharlesX. The axial flame height and radial length were overpredicted by a factor greater than 2, and this was also followed by thicker flame branches and insufficient distribution of the heat release on the borders of the CRZ. Paulhiac et al. [104] showed that for *n*-heptane, the overall flame shape (semi-quantitative) had good agreement with the experimental data. Nevertheless, the flame height from the top of the bluff-body to the centre of the M−shape was reported to be overpredicted by a factor of 2.33, while significant misprediction of heat release level at the edges of the bluff-body appeared to be inconsistent with the experimental results.

The Cambridge biofuel swirl burner

The Cambridge biodiesel swirl burner has recently been investigated by Mohd Yasin et al. [91], focusing on modelling a composite of biodiesel (Palm Methyl Ester-PME) by including the volatility of the several different fuel components. This was accomplished by developing and applying a discrete multi-component biodiesel (DM) model. The results were compared against the traditional Continuous Thermodynamics model (CTM). The CFD solver OpenFoam by means of the standard unsteady-RANS-k-ε model was used with an Eulerian-Lagrangian two-coupling approach. The combustion (turbulence-chemistry) was modelled using the Chalmers Partially Stirred Reactor (PaSR) approach as proposed in Kärrholm [63]. The main drawback of this approach is that it assumes that a real flame is much thinner than any computational cell, thus assuming that each cell is a perfect reactor which is considered a severe overestimation because all present species are considered homogeneously mixed and reacted while the chemical source term is laminar [63].

In the establishment of the inflow boundary conditions, the swirl device was not included in the computational domain, therefore the three-inlet velocity components were estimated from the air mass flow rate, and the tangential velocity was obtained algebraically from the geometry swirl definition of Beér and Chigier [7]; validation of the non-reacting swirling flow in terms of the mean velocity profiles and turbulence quantities (turbulent kinetic energy and flow structures) in the central recirculation zone was not performed. Because data were only measured at a distance of 10 mm from the inlet exit, a clear definition of the turbulence initialisation parameters was not achieved. The spray boundary conditions were set using a Rosin-Rammler droplet size distribution, but no information regarding the number of parcels selected was provided; the convergence and numerical stability of the Lagrangian solver were not investigated.

The CFD results indicated a 20 % overestimation of the droplet

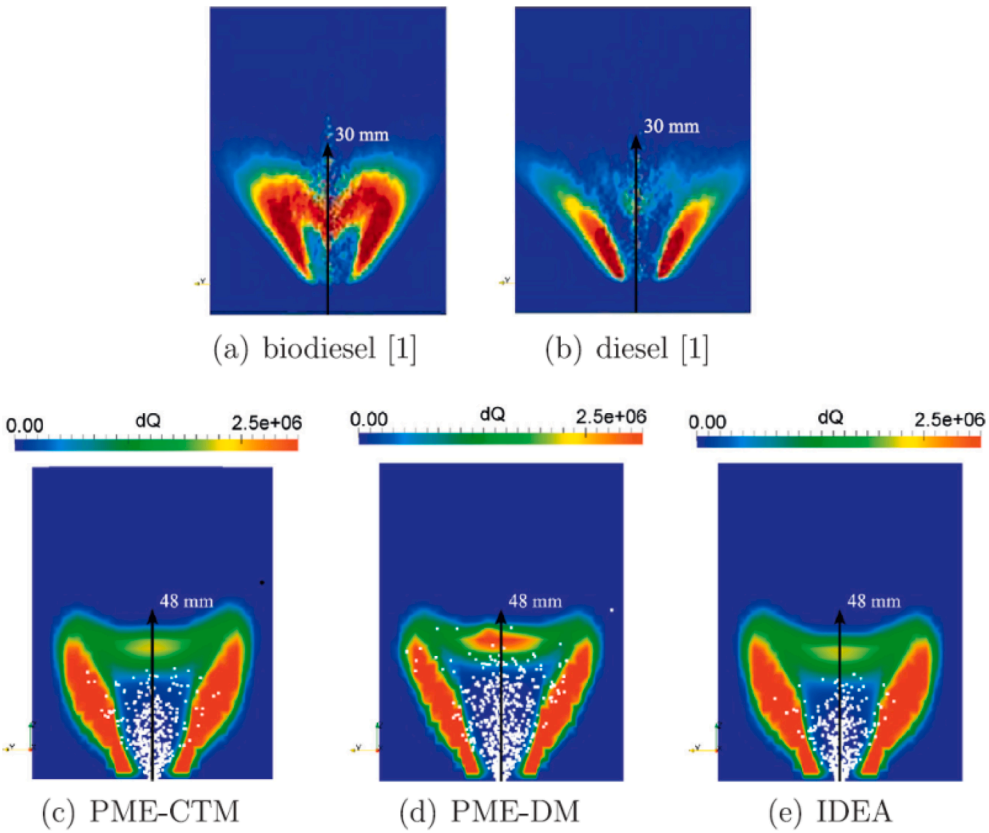

Fig. 4-4. Quantitative comparison of the predicted flame heat release (bottom row) using the three different liquid models (c) PME-CTM, (d) PME-DM and (e) IDEA against the (top row) experimental Abel-transformed *OH** chemiluminescence data for (a) biodiesel and (b) diesel Mohd Yasin et al. [91].

properties such as size, volume-flux and density and most of the changes in the droplet size were not reproduced according to the experimental database. These were associated with inaccuracies in the spray boundary condition, mostly because the establishment of the spray boundary cannot be accomplished fully because the size of the droplets was only measured at 10 mm above the injector nozzle.

Fig. 4-4 shows the experimental (top row) *CH** chemiluminescence data for botiodiesel and diesel and the semi-quantitative predicted CFD heat release results (bottom row) using the three different liquid models. Regardless of the liquid spray model chosen in Fig. 4-4 (c), (d) and (e), the maximum simulated flame height values were around 48 mm, which overpredicted the experimental value (30 mm) by 18 mm. Although none of the simulated heat release shape outcomes agreed with the experimental data, it is still possible to say that the discrete particle models (DM) could quantitatively reproduce the heat release of biodiesel flame that appears in the central region of the CRZ linking the two flame brushes, thus justifying the possibility of improving this approach in future studies. None of the models was capable of reproducing the features expected for diesel. Moreover, the spray penetration is longer for the PME-DM, evidencing substantial changes in evaporation; this region is strongly affected by the recirculation air and by a high rate of evaporation; the side of the M shape is overall narrower than the experimental data of biodiesel. Since different combustion and turbulence models were not compared, one cannot discern how much of these mismatches come from the turbulence-chemistry interaction and the two-way coupling approaches. Only the uncertainties and interferences coming from the spray boundary are documented. No attempts to validate the flame lift-off were made on the basis that experimental measurements were not available. Nevertheless, one can visually note in Fig. 4-4 (a) and (b) that both biodiesel and diesel have a lift-off distance from the bottom of the burner, while the numerical results in Fig. 4-4 (c), (d) and (e) indicate flames attached to the burner bottom.

The DLR burner

Numerical studies based on the experimental data from the DLR burner have been carried out. An in-house Lagrangian tracking code developed by the DLR called Spraysim was used to track the droplets and compute evaporation rates in conjunction with an evaporation model based on the model of Abramzon and Sirignano [1]. The validity of this evaporation model was discussed in Rauch et al. [121]. In order to have a balanced comparison between different fuels, the initial temperatures and droplet diameters of all the fuels were kept identical. It was noted that these might differ depending on the fuel type. Two fundamental chemical kinetics properties, laminar premixed flame speed and ignition delay time were solved by using the Chemical WorkBench 4.0 solver. Laminar flame speeds were calculated using initial fuel-oxidiser composition, temperature and pressure. A multicomponent transport model was used to calculate the flame, taking into consideration thermal diffusion. Ignition delay times were computed based on a zero-dimensional homogeneous constant volume reactor model with the initial mixture composition and the initial temperature and pressure behind the reflected shock wave as inputs.

Additionally, the DLR reaction kinetic database was used for the fuel reaction mechanisms Kathrotia et al. [64]. This numerical study concluded a strong similarity in atomisation and vaporisation properties between *n*-hexane and isooctane; however, their chemical kinetics differed noticeably. It was also reported that the vaporisation and atomisation properties of *n*-dodecane were significantly different to that of the other two fuels. The chemical kinetic results showed a similarity between *n*-dodecane and *n*-hexane. It was also noted that *n*-hexane exhibited better extinction performance compared to *n*-dodecane.

The DLR swirl-stabilised spray burner has also been simulated using multi-component fuel by Eckel et al. [29]. In this study, the LES approach is used to study the interaction between a multi-component vaporisation model and a direct, detailed gas-phase chemistry solver.

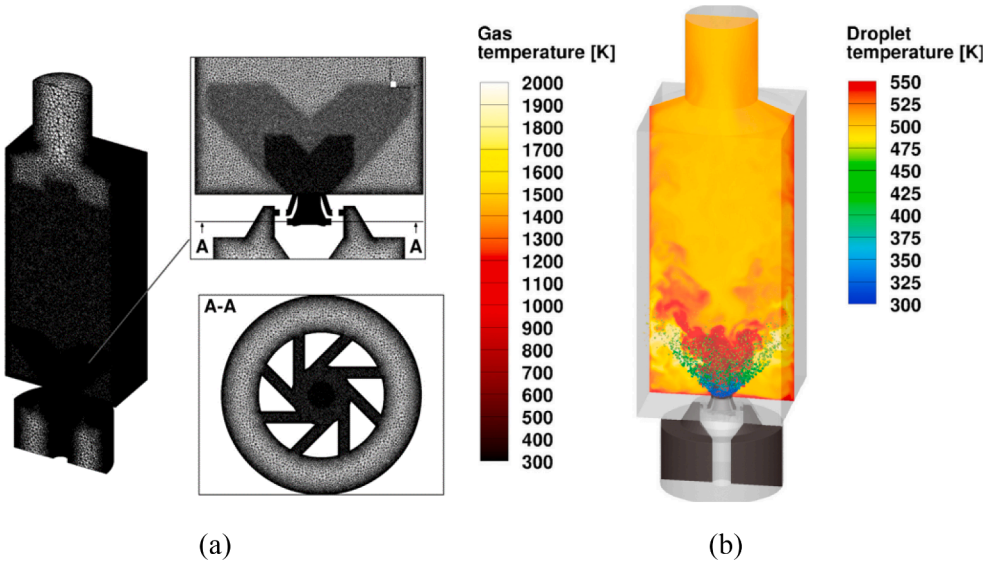

Fig. 4-5. (a) The computational domain is discretised with high clustering of elements in the flame and spray zones - the darker areas, (b) shows a typical flame structure superimposed by the temperature of the droplet Eckel et al. [29].

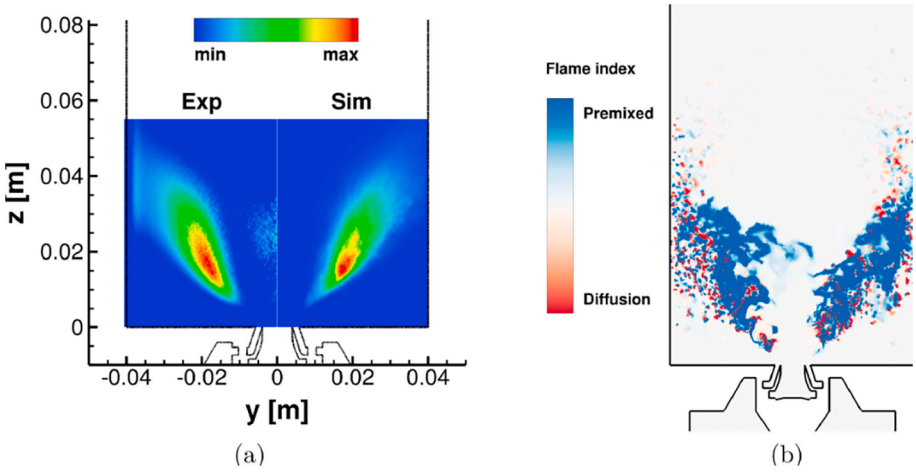

Fig. 4-6. (a) Comparison between time-averaged CH*-Chemiluminescence (Abel-deconvoluted) (left) and time-averaged OH*-distribution predicted with LES (right); (b) is the flame index to identify the flame multimode (premixed and non-premixed) regions Eckel et al. [29].

The gaseous phase was modelled using a finite volume solver in the Eulerian frame of reference, whereas the liquid phase was solved using the Lagrangian particle tracking method using the point source approximation. The gas solver is called THETA. The pressure–velocity coupling is carried out on a projection method, while the Poisson equation for the pressure correction is solved using the technique; both the convective and diffusive fluxes are computed using a second-order Crank-Nicolson scheme while the time discretisation is carried out using a second-order, low-dissipation and low-dispersion central scheme. The other transport equation was solved using the BICStab method with a Jacobi preconditioning Eckel et al. [29].

In this study Eckel et al. [29] the fuel and oxidiser boundary conditions for the simulations were derived from the experimental study by Grohmann et al. [43]. Regardless of the computational cost, the swirl device was included in the numerical domain; thus, mitigating numerical uncertainties by using decomposed domains or inlet with constant and arbitrary velocity profiles. The number of computational parcels used in the discretisation of the Lagrangian solver was not informed, and numerical convergence and stability criteria were not explored; therefore, numerical inaccuracies coming from the spray boundary condition could not be ruled out. Since the wall temperature is known, they ascribed the temperature for the bottom plate, including the central part (717 K), the glowing ring (901 K) and the corner of the bottom plate 831 K, the side windows are at 1205 K, and the other surfaces considered adiabatic Nau et al. [93].

Fig. 4-5 (a) shows the fully unstructured tetrahedral mesh used in this study; the mesh size for the computational model is 14.7 million points which corresponds to 80.7 million tetrahedral cells. The mesh is refined in areas of interest such as the region in the proximity of the flame, near-wall regions, mixing zones and swirler vanes. It was reported that the ratio of the turbulent and molecular viscosity in non-reacting fundamental investigations influenced this choice of refinement. Fig. 4-5 (b) shows an instantaneous snapshot of the gas and droplet temperature results evidencing the matching of grid refinement zones with the area where combustion takes place.

The validation of the non-reacting time-averaged velocity profiles (axial, radial and tangential) matched the experimental data. As observed in Fig. 4-7 (a) the flame global features ('V' shape) as revealed by the position of the reaction zone were well-captured by the numerical modelling. However, the experimental data revealed a more elongated region with maximum CH*-chemiluminescence distribution (reddish shade) in the shear layer, while the maximum LES OH-distribution

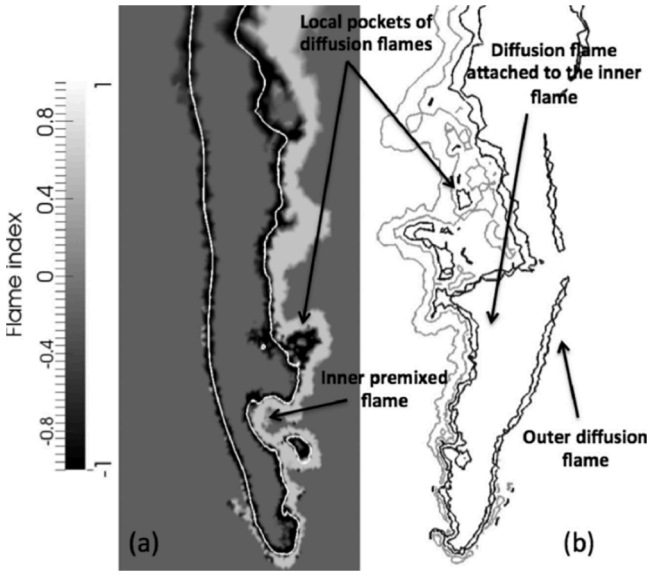

Fig. 4-7. Flame structure as revealed by the Takeno flame index (a) and the isolines of Takeno flame index; premixed flame (grey) and diffusive flames (black) (Shum-Kivan et al. [135]).

profiles are shorter and compact. It is believed that the spray boundary condition affected this result. As observed in Fig. 4-6 (b), the flame is predominantly premixed and occurrs in a region enhanced by highly turbulent flow (at the inner part of the flame zone) while the appearance of non-premixed flame modes are scattered across regions around the outer edges of the flame towards the confinements. The maximum experimental temperature achieved was 1820 K, while the numerical methods computed this as 1730 K; at the centre of the CRZ, the temperature was underestimated by a factor up to 1.4; according to Eckel et al. [29], these discrepancies were attributed to issues in defining the temperature boundary condition and uncertainties with spray boundary conditions.

Quantities such as the droplet size, droplet velocity and liquid flux showed satisfactory agreement with experimental data. It was concluded that further numerical studies would be required for complete validity. One of the drawbacks of this study was the necessity of solving the finite-rate chemistry model (FRC). In other words, transport equations had to be solved for each species (80 species) in the chemical reactions (464 reactions) on 80.7 million grid points; this gives an additional set of 80 equations per each time step; the computational cost and numerical strategy to overcome the stiffness on solving the non-linear Arrhenius equations were not reported in Eckel et al. [29].

Unconfined burners

The CORIA jet spray

The numerical modelling of this flame was carried out by Shum-Kivan et al. [135], who used a combination of LES coupled to the Discrete Particle Simulation (DPS) and the two-way coupling approach between the liquid and continuous phases. The main goal was to provide insights into the turbulent flame structures by looking at the interactions between droplets and flame. The CFD solver used was the compressible AVBP solver [134] developed by CERFACS, and the discretisation schemes are 3rd order in both time and space. The Chemistry reaction was modelled using a simplified two-step global reaction tested on laminar premixed flames under ambient conditions.

The geometry of the entire burner was simulated; this was feasible because the burner has no swirl vanes and moving parts; therefore, only one velocity component (axial) is created; the meshing of the inlet pipe, the cylindrical plenum and injection veins required 53 million of tetrahedral cells. The non-reacting flow air was validated against the mean and rms of axial velocity, for which a satisfactory match against experimental data was achieved. In the establishment of the spray boundary conditions, the liquid phase was considered dispersed, and the assumption of an already formed (diluted) spray was applied. The spray velocity and size distribution were obtained from the geometrical characteristics of the injector. Sensitivity studies involving these parameters and validation against cold droplets size distribution at the first measurement station (Z = 13 mm) were not presented; the number of computational droplets used at the dispersed phase boundary condition was not presented, and the convergence and stability criterion of the DPS solver was not assessed.

Fig. 4-7 reveals the combustion regime captured by CFD using the Takeno flame index. This result can be used in comparative studies involving different CFD platforms and combustion models. The evaporation process creates inhomogeneities in the flame, which is followed by an intriguing behaviour combining both diffusive (outer edge region) and premixed flame (inner region) with several random pockets of both regimes distributed across the flame volume; this is a typical and complex phenomenon in spray flames [135]. The results for droplets size radial distribution indicated that larger inertial droplets were found on the external part of the spray; however, some discrepancies (errors outside the experimental error bars) in the axial and radial velocities of the larger droplets were attributed to a lack of statistical convergence resulting from the low number of droplets in the simulation. The experimental flame lift-off was 25 mm, while the LES result was reported to be shorter, but no values were informed on the basis that the results were under investigation [135]. Further details on the limitations and uncertainties of the combustion model were not discussed.

The delft spray burner

The numerical analysis of the piloted non-swirling unconfined DSHC experiment (section The Delft Spray-In-Hot-Coflow (DSHC) spray burner) was carried out by Ma et al. [81], Ma et al. [80], Ma and Roekaerts [79] and Ma [78]. The authors had previously investigated this experiment using different simulation models; for instance, URANS with fully adiabatic steady laminar flamelets [81] and Ma [78], and Lagrangian-Lagrangian PDF [80] and LES/FGM with non-adiabatic flamelets using non-premixed reactors Ma and Roekaerts [79]. Non-swirling air inflow boundary conditions were initialised using the measured velocity profiles (axial and radial) at the first measurements station (Z = 8 mm), where diluted conditions were achieved, thus avoiding the dense spray area. The spray boundary condition was estimated from 2D-URANS-k-ε calculations coupled with the Linearized Instability Sheet Atomisation (LISA) model; the droplet size distributions were numerically estimated at the first measurement station (Z = 8 mm) and interpolated into a three-dimensional (3D) computational domain; this was necessary to avoid the dense spray region. An assessment of the stability and convergence criteria achieved by the Lagrangian solver were not explored.

By using a 2D-URANS-k-ε with a steady-state adiabatic laminar flamelet method within ANSYS Fluent®, the main failure identified was the model's inability to predict the flame lift-off phenomenon when compared to the experimental *OH*-distribution, in fact, the flame initiated immediately downstream the injector, and this was attributed to the fact that the effects of heat loss/gain that were neglected on the species mass fraction as well as the model led to too early ignition which in turn caused deviations in droplet axial velocity [81] and Ma [78]. A second simulation using an in-house Lagrangian-Lagrangian PDF code was carried out with a fully adiabatic non-premixed FGM model, and the results revealed that the gas temperature at the centre of the burner was under-predicted (approximately by 200 K) while the temperature RMS was overpredicted by approximately 100 K, especially in flame regions where enthalpy loss due to evaporation was expected; this was attributed to the lack of heat loss in the flamelet table and the lack of temperature fluctuations boundary conditions at the inlet [80] and Ma [78].

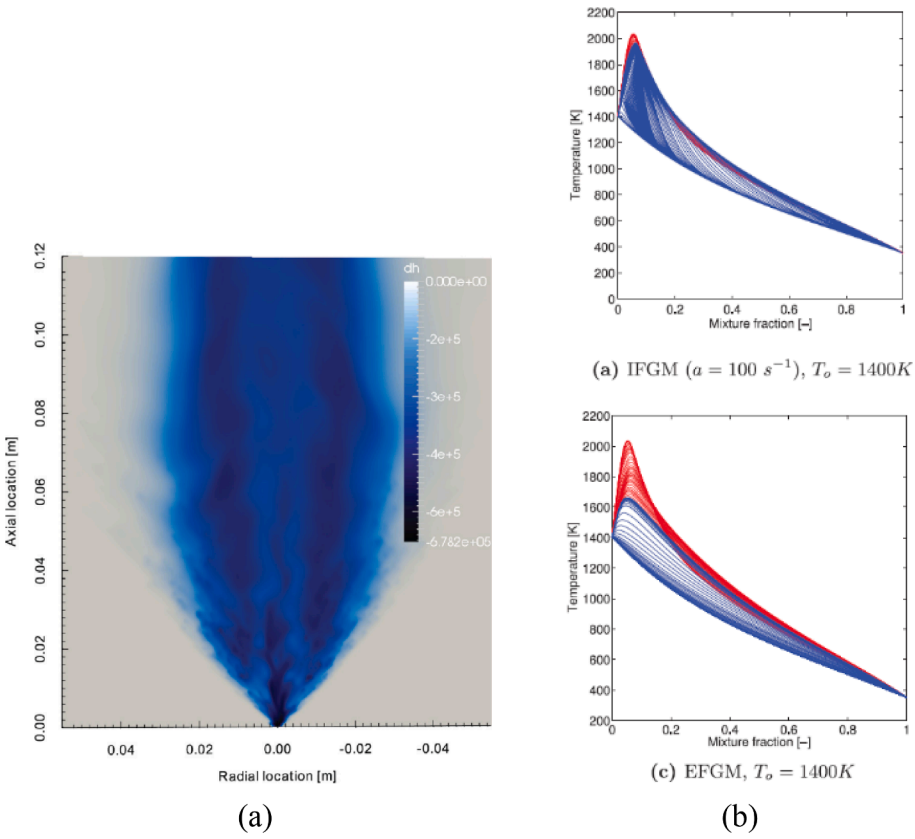

Fig. 4-8. (a) Typical enthalpy deficit generated by the non-adiabatic FGM table; (b) typical temperature in mixture space generated using the IFMG and EFGM method using a constant scalar dissipation value for steady (red line) and unsteady Flamelet Ma and Roekaerts [79].

This temperature issue was further investigated by Ma and Roekaerts [79] and Ma [78] by using a non-adiabatic FGM table to account for the evaporation effect (enthalpy loss) associated with the evaporation phase in the FGM equations within LES. The enthalpy loss in the FGM library was generated considering two different types of chemical reactors, a non-premixed ignition FGM (IFGM) and extinguishing FGM (EFGM) effects for different levels of normalized heat loss. A typical outcome for the enthalpy deficit is shown in Fig. 4-8 as well as a comparison between the steady and unsteady Flamelet models evidencing the decrease in temperature due to enthalpy loss in both IFGM and EFGM.

The authors observed that both the IFGM and EFMG were strongly influenced by the strain rate. Both methods have pros and cons that can drastically influence the analysis of turbulent spray flames. For instance, for both low/high strain rates, the IFGM/EFGM underestimated the peak of temperature for all axial locations considered; this was attributed to issues in modelling the mixture fraction variance; at the centre of the burner, the temperature estimated with the EFGM was comparable to the experimental value while the IFGM under-estimated this (depending on the radial location) by a factor up to 1.75. The temperature profile was sensitive to the strain rate used in the flamelet generation; therefore, depending on the strain rate value for both methods, they can give quite similar or different results because of the impact on flame ignition. Furthermore, comparisons between the mean gas-phase velocity using both URANS and LES showed that the results were similar, thus supporting the reliability of the use of URANS for this type of flame; in terms of the mean temperature value, the LES predicted the peaks better, and this was attributed to better performance of the mixture fraction variance model adopted in the LES model [79].

To overcome difficulties in defining a suitable chemical reactor for FGM spray table generation, Ma and Roekaerts [79] raised the possibility of choosing a different chemical reactor in constructing the FGM manifold; in this case, they suggested using the Igniting Mixing Layer (IML) method applied in Abtahizadeh et al. [3]. According to Abtahizadeh [4] and Abtahizadeh et al. [3,2], this method is similar to one-dimensional igniting diffusion flamelets, and the main assumption of this method is that a situation of perfect-mixing (molecular mixing) can occur between the fuel and oxidiser even before any chemical reactions take place. Mixing is achieved when a turbulent shear layer (due to Kelvin-Helmholtz instabilities) is formed between the fuel and the hot recirculating air. The second assumption is that the mixture is homogenous, and there is no gradient of mixture fraction. The third assumption establishes that due to the absence of an applied strain, both species and temperature approach chemical equilibrium for an infinite time. Therefore, chemical reactions may start at any time during the mixing process; in other words, the flame is autoigniting. Other types of perfectly mixed homogenous igniting reactors were presented in Turns [139], and they share similar assumptions with the IML approach. According to Ma and Roekaerts [79], it is believed that this approach would improve the accuracy of ignition and temperature predictions in burners under spray combustion conditions.

Finally, because a surrounding piloted burner stabilises the flame, the experimental data revealed that flash boiling phenomena caused by the superheating of the fuel liquid had generated vapour bubbles, which expanded and exploded, accelerating the atomisation process. Ma and Roekaerts [79] explored this phenomenon and suggested that traditional atomisation models, such as LISA (Linearized instability Sheet Atomisation), were no longer valid for this MILD combustion application. However, the effects of flash boiling on actual flame results were not fully explored.

The Sydney spray burner

The piloted Sydney spray burner (Fig. 2-7) is the basis for most simulations reported in the literature; mostly because the implementation of boundary conditions is simplified, and the geometry and meshing

Table 2
-1. Summary of historical spray burner platforms - Alcohols.

Burner platform	Aims, burner and phenomena type	Cold and reacting flow measurements and assessments
University of California (UC) Irvine Swirl Spray Burner McDonell et al. [86], McDonell and Samulsen [89]	Experimental database for CFD modelling development and validation. Three different ranges of fuel injector operation (with no atomiser air, non-swirling atomiser air and swirling atomising air)	The bulk air velocity and fuel flow rate, and temperature for all cases are reported. Phase Doppler-Interferometry (PDI) is employed for the measurements of gas-phase velocity in the presence of a sprayMcDonell and Samulsen [88]. Measurements start at 7.5 mm downstream of the tip of the injector.
	The burner is composed of a square duct. The atomizer used is a Parker Hannifin Research Simplex-Air (RSA).	Photographs were taken to show the global structures (both non-reacting and reacting cases). The droplets size distribution is presented for the non-reacting case. Reacting case is available in McDonell and Samulsen [87]. The impact of different injection modes (swirling atomising air and no atomising air) is quantitatively compared.
	The swirling methanol spray flame is stable and considered soot free. Both the chemical kinetics and thermo-data are available in the NIST webbook (United States (US) Secretary of Commerce [146].	For the reacting case, discrimination of the momentum transfer between the phases was not possible due to continuous changing of the droplet size. Vapour concentration is measured using an Infrared Extinction and Scattering (IRES) system Adachi et al. [5]. Methanol vapour percentage is superimposed with gas-phase velocity vectors for all the cases analysed. Uncertainty (for non-reacting mass conservation measurements) is presented for the liquid flow using PDI, vapour flow using IRES and a combination of both PDI and IRES methods for the total flow rate of vapour.
Yale Prevaporized Spray Burner	A spray system is designed with a turbulence enhanced scheme on the oxidiser side, and droplets are imparted with minimal velocity. Boundaries conditions are reported only for the reacting case, which can be used for CFD.	PDA is used for measurements of droplets velocity, velocity correlation and size, as well as axial and radial gas-phase velocities (average and fluctuating)
[60–61,59]	The burner is unconfined and non-swirling, and turbulence is synthesised using a perforated plate and contoured geometry. Geometrical dimensions are limited. A commercial ultrasonic nebuliser (Sonotek) is used for atomisation. Methanol is used. Two stable and anchored brush type flames, namely flame I (airflow rate of 80 L/min) and II (110 L/min), both with an overall equivalence ratio of 0.35 and 0.15, respectively.	There is a minimum slip velocity between the droplets and the carrier air close to the tip of the atomiser. Droplets have an average diameter of 30 μm. Gas temperature (average and fluctuating) is measured using spontaneous Raman thermometry as in [62]. High local temperature fluctuations are associated with the inherent intermittency of the spray and might be driven by the individual burning of droplets.
		A self-similarity study is presented to describe the spray flame as a combination of a point source of momentum and a vaporisation approach. Chemiluminescence images of CH* (150-μs exposure time) are provided for the qualitative analysis of flame morphology as inKarpetis and Gomez (2000.
National Institute of Standards and Technology (NIST)	Experimental database for CFD modelling development and validation.	Air inlet velocity magnitude and turbulence intensity profiles are measured using Particle Image Velocimetry (PIV); the data are available in Widmann et al. [152]
Benchmark Spray Database	Relevant dimensions and information on the enclosed burner and combustion chamber, swirl device and atomizer are available.	Fuel flow rate and pressure; Gas velocity at different axial stations. Wall temperature. Two dimensional (2D)-PDI at seven elevations are used for droplet size, number density and velocity distributions which are accompanied by uncertainty analysis. Fourier Transform Infrared (FTIR) spectroscopy is used for concentration measurement of CO, CO_2 and CH_3OH at the outlet
Widmann et al. [151], Widmann et al. [153], Widmann and Presser [154]	The swirl spray flame is stable and burns methanol. Both the chemical kinetics and thermo-data are available in U.S. Secretary of Commerce [146].	
Heidelberg Burner Düwel et al. [27]	Experimental database to characterise spray flame for validation of numerical codes. This burner was initially developed at UC Berkeley see Cabra et al. [15].	Fuel flow rate (0.39–0.54 g/s) and the co-flow air velocity (0–0.64 m/s) are reported. Three different injection pressure values are used (1.4, 2.0 and 2.4 bar). The flame has two zones. The inner zone starts just 1 mm above the nozzle and the outer from 5 to 15 mm above the nozzle.
	The burner is unconfined and non-swirling; the liquid is injected using a hollow-cone spray nozzle (Delavan 67700–5). The main dimensions are available. The flame operates in a stable mode (without bluff-body or pilot flame), burning ethanol fuel. A homogenous co-flowing air is not pre-heated. Ethanol is pre-heated to 45C.	Sauter mean diameter (SMD) is measured using both Mie/LIF-drop sizing and PDA for reacting spray droplets, which is also used for velocity measurements. The 2-D contour of SMD is presented.

(continued on next page)

Table 2 (*continued*)

Burner platform	Aims, burner and phenomena type	Cold and reacting flow measurements and assessments
		2-D contour plots of liquid-phase temperature are obtained by 2-color LIF temperature with Rhodamine B. The gas-phase temperature using NO-LIF temperature imaging is available in 2-D contours and profiles at four different stations. Measurements are obtained near the nozzle (just 2 mm downstream) to establish numerical conditions. Radial velocity in the vicinity of the nozzle is measured with an error of 10%.

are simpler compared to aeronautical swirl-burners akin to gas-turbines; hence, the geometry for CFD domains usually starts from the exit of the burners hence requiring less CAD effort because it does not use swirl vanes and enclosed domains; the entire burner including the tangential air inflow ports are not included in these numerical simulations. In addition, flame stabilisation is achieved using a piloted flame, and this facilitates the evaporation and ignition processes.

A non-exhaustive yet detailed summary of the various numerical studies based on the Sydney spray burner is thus presented in Table 4-1. Emphasis was given to detailing the turbulence and combustion models adopted, the fuel and chemistry mechanisms applied, and a detailed assessment of the combustion outcomes were reported and critiqued. The CFD results from the different methods in Table 4-1 show that many questions are still open even for a more straightforward burner, especially regarding the accuracy and limitations of the combustion models adopted. From RANS models, it is possible to see that the primary deficiencies come from modelling the turbulent interactions. While the issues and inefficiencies in solving the spray combustion with LES using either flamelets, FGM and conditional methods were attributed to lack of non-adiabatic effects in generating the chemistry tables and inappropriateness in establishing inflow boundary conditions and lack of consensus in selecting the chemistry reactors for flamelet generation.

Summary of computational studies for burners in Tables 2-1 and 2-2

A non-exhaustive summary of the numerical simulations for the historical burners (Table 2-1 and Table 2-2) is now presented in Table 4-2, focusing on turbulence and combustion modelling employed, assessment of boundary conditions implementation issues, and combustion outcomes assessments. As far as this review is concerned, the following burners were not investigated using CFD methods: the Imperial College Swirl Spray [44], the SANDIA Swirl-Stabilised Spray Flame [28] and NASA Swirl Burner [14,13]; hence, they were omitted in Table 4-2.

In summary, turbulence modelling was mainly performed using steady-state RANS closed with the isotropic k-ε model, while some recent studies used LES. There were no investigations with URANS closed with Reynolds Stress modelling. Swirl inflow conditions were mainly performed using imposed uniform inlet velocity profiles and extrapolated velocities obtained from experimental data inside the combustor section; attempts to derive more accurate boundary conditions were not performed. Studies of the impact of the number of computational parcels on the Lagrangian boundary conditions and convergence/stability analysis were not performed. There was a predominance for combustion modelling based on flamelets (especially the Flamelet Generated Manifold - FGM). Overall, FGM tables were generated using fully adiabatic tables primarily based on non-premixed chemistry reactors and reduced chemical mechanisms, while the

Table 2
-2. Summary of historical spray burner platforms – Fossil fuels.

Burner platform	Aims, burner and phenomena type	Cold and reacting flow measurements and assessments
Imperial College Swirl Spray Burner Hardalupas et al. [44]	Understanding the underlying physics of stable kerosene spray flame. Boundaries conditions are reported for both non-reacting and reacting flows which can be used for CFD modelling and validation. Unconfined quarl swirl burner (furnace-type) assisted by a natural gas flame. Liquid fuel is injected using an air-blaster atomiser. Swirl is aerodynamically created by tangential ports.	PDA is applied for droplet size and velocity measurement as well as for the mean air velocity profiles for the non-reacting case, which were measured at the exit of the burner contraction. The flow is asymmetric. The burner provides a thermal power of 21.6 kW and 37.2 kW for an equivalence ratio of 1.21 and 2.11.
	The stable flame was studied and measured. The influence of the aerodynamics response of different droplets' size and two different kerosene flow rates on the flame physics were assessed.	Evaporation and burning rates are indirectly assessed at the exit of the quarl (at the inner and outer edges of the spray) by evaluating the changes in the droplet size.
		Droplets burnt following the 'Cloud burning' within the combustion group classification. Droplets evaporated quickly in regions of high temperature; therefore, no droplets were found in the inner flame branch and the internal recirculation zone. The mean air velocity towards the central recirculation induced by the 30 μm or smaller droplets is entrained by the mean air velocity. Droplets greater than 60 μm can escape the central recirculation zone and are unaffected by turbulence fluctuation.
SANDIA Swirl-Stabilised Burner	The experimental database was generated for numerical modelling validation.	Mean gas-phase velocity vector data in the axial/radial plane are measured using single component Laser Doppler Velocimetry (LDV). However, it is only accurate for an axial location up to 25 mm due to limitations in signal acquisition. Two-component PDA (Phase Doppler Anemometer) is used to measure the droplet's size and velocity. Spray velocity vectors are plotted in the axial and radial planes. The burner generates a thermal power output of approximately 60 kW for a fuel flow rate equal to 1.4 g/s.
Edwards and Rudoff [28]	The research burner is a furnace (octagonal cross-sectional area) with a swirl device. The walls are made of fused silica (quartz) to allow optical diagnostics.	Both flame and liquid structures near the injector (dense phase) are assessed using Schlieren photographs. The primary flame zone occurs at about

(*continued on next page*)

Table 2 (*continued*)

Burner platform	Aims, burner and phenomena type	Cold and reacting flow measurements and assessments
	The atomizer is a Parker Hannifin Research Simplex-Air (RSA).	one-third of the combustor length. A combination of multiple measurement techniques (Schlieren, luminosity and extinction imaging) are used to capture the internal boundaries encompassing the flame, the dense spray zone, and the external recirculation zone. Therefore, it can be used for qualitative comparison with CFD data.
	The macro-structure of a stable kerosene flame is investigated in a confined and highly swirling environment, accounting for analysis in the near-injector region.	
Imperial College	Generation of spray flame database for CFD modelling development and validation.	The flame mean and root mean square (RMS) temperature distribution for different axial locations are measured. Therefore, it indirectly allows the analysis of droplets evaporation and motion within the flame.
Swirl-Stabilized Axisymmetric Model Combustor Sheen [136]	A confined cylindrical chamber with a sudden expansion; highly swirling environment with a strong recirculation zone to mimic gas-turbine combustors. Stable spray flame burning aviation kerosene (Jet-A). A second flame close to the blow-off limit was investigated.	Measurements of droplet size and velocity distributions were not carried out.
NASA Swirl Spray Burner Bulzan [14,13]	This burner is intended to generate a measurement database of droplet size and velocity for a reacting spray burner.	Both mean and RMS of the velocity and fluctuating velocity profiles (axial, tangential and radial) of the gas-phase and droplets are measured using a two-component PDA system at 6 different downstream traverse locations.
	The burner is confined with swirling imparted air. The liquid is injected using a Parker Hannifin Research Simplex-Air (RSA) atomizer. The flame operates in a stable mode (swirl-stabilised), burning heptane fuel. Co-flowing air is not pre-heated.	Air and fuel flow rates are reported. Droplets number fluxes (for six drop sizes) are measured. Uncertainty analysis is presented for measurements of fuel and airflow rates, probe position, gas-phase velocity, drop size and number-flux. The flame temperature and species mass fraction measurements are not carried out.
CNRS Orleans Burner Pichard et al. [111]	Experimental database of partially pre-vaporised and premixed spray flames for CFD modelling and development. The research burner is an enclosed tube where pre-vaporisation and mixing occur; combustion is assisted by a pilot methane/air flame, which takes place	Fuel and airflow rate and the Sauter mean diameter are reported for the three equivalence ratios investigated. PDA is used in the measurement of two-component droplet axial and radial velocities as well as to obtain droplets sizes. The co-

Table 2 (*continued*)

Burner platform	Aims, burner and phenomena type	Cold and reacting flow measurements and assessments
	at the exit of the tube in the open section (unconfined). The burner dimensions are available. An air-assisted atomiser is used. The co-flow is non-swirling and turbulent. The stable flame comes from a pre-vaporized *n*-heptane/air mixture.	flowing airflow rate is kept constant and equal to 1.66 g/s, while the initial droplet diameter can be changed.
		PLIF is used to determine the instantaneous flame front position and isocontours of the progress variables. The average vaporisation ratio is computed and presented from the PDA measurements considering three different equivalence ratios. Experimental uncertainties are estimated to be 8% droplet diameter, 10% SMD, 20% droplet number density and 3% for mean droplet axial velocity.

selection of progress variable species coefficients was usually arbitrary. In some cases, stratification effects of the mixture fraction were not properly resolved; inflow conditions were mostly generated using uniform flow properties without the presence of the swirl device, thus, leading to the lack of turbulence information at the inflow boundary. Attempts at using the Conditional Momentum Closure – CMC have relied on using one and bi-dimensional chemical tables without including heat loss effects.

Main research gaps in the CFD modelling

A considerable number of CFD studies have been carried out in modelling the swirl spray combustion of the burners presented in section Types of burners. However, most of the numerical modelling uncertainties and inaccuracies in these studies and their implications on spray flame outcomes can be attributed to broadly-six issues below identified by this review study.

Firstly, there are unresolved issues attributed to turbulence modelling of the swirling non-reacting flow; especially due to inappropriate establishment of swirl inflow boundary conditions and lack of methodology for the selection of the turbulence modelling to capture the high anisotropy effects in the central recirculation zone and shear layers. These are important for resolving the central recirculation zone, and hence, for example, the placement of the injector and or ignitor.

Secondly, there are unexplored issues attributed to the Lagrangian solver used in the popular commercial and in-house CFD codes, mainly due to the lack of a methodology and or a consensus in prescribing the appropriate number of initial computational droplet parcels at the spray boundary conditions, followed by a lack of methodology for the solver validation and convergence/stability criteria.

Further to the point identified above, the unexplored impact of the number of initially prescribed computational droplet parcels on the actual spray flame ought to be investigated because the flame mode is sensitive to the spray evaporation and droplets dynamics. Moreover, previous studies did not benchmark their CFD results against other non-Lagrangian CFD solvers. Hence, in the long term, the progress in the field is retarded, and this source of uncertainties and inaccuracies in the numerical results remain, as shown from results in section

Table 4
-1. Summary of modelling studies of the piloted Sydney spray burner.

Study/ Precursor studies	Details: turbulence and combustion models	Fuel & chemistry mechanism	Lagrangian solver and Combustion assessments
[142]/ [142–144]	LES with a dynamic Smagorinsky model Germano et al. [37] and Branley and Jones [9]. An extended CMC technique (CMCe) was coupled with tabulated chemistry, similar to that in Kronenburg and Kostka [68]. A spray source term is added in the CMCe equations. A 2-D fully adiabatic Flamelet Generated Manifold (FGM) approach is used to tabulate the chemistry table space using unsteady 0-dimensional CMC equations. The combustion modelling is entirely non-premixed; progress variable species coefficients are inconsistent for Acetone because it came from methane/air gaseous flame of Ihme and Pitsch [50].	Acetone with two different injection rates. Acetone mechanism consists of 416 reactions and 81 species Pichon et al. [112].	Studies of the Lagrangian solver boundary conditions and validation were not performed. Improved temperature value predictions were found whilst comparing against conventional CMC modelling [145] mainly along the burner's centreline, where the effects of evaporation significantly increased the conditional fluctuations.
[22]/ [21,23–24]	LES with a Dynamics-Smagorinsky model [37] coupled with a Lagrangian droplet dynamic model was used to numerically study ethanol spray flames with boundary conditions for cases EtF3 and EtF8. The LES code FASTEST3D [132,149,76] was used to discretise the gas-phase equations while the LAG3D code [132] was used to track parcels. Evaporation is modelled using the Uniform Temperature (UT) model by Abramzon and Srignano [1]. The combustion was modelled using fully adiabatic FGM tabulated chemistry generated with a one-dimensional non-premixed reactor; progress variable species coefficients were arbitrarily used.	Ethanol with 56 species and 351 reactions Marinov [83].	Validation studies of the LAG3D solver in terms of the number of parcels and the convergence/stability were not performed. Combustion properties such as flame height were considered reasonably predicted. The integration of heat losses into the FGM approach was recommended as heat loss due to evaporation is vital for droplet phase transition close to the nozzle exit. Further investigations into the influence of four-ways coupling near the nozzle exit region as well as the dispersion modelling impact on droplet diameter distribution were recommended.
[45]	LES was performed on turbulent spray with boundary conditions based on case EtF1 in Masri and Gounder [85]. A PDF transport equation was developed for the multi-scalar problems. Additionally, a Lagrangian solution methodology was developed for low-Mach number combustion. The resulting LES/PDF approach was used in this study. Combustion is modelled with a fully adiabatic flamelet/ progress variable-based combustion model coupled with the transport pdf approach. The progress variable species coefficients and the chemical reactor applied were not informed.	Ethanol with 50 species and 235 [141].	Sensitive studies of the Lagrangian boundary condition, convergence and numerical stability were not performed. Qualitative comparisons between the experimental study and the LES/PDF simulation were reported. The significant discrepancies between the numerical and experimental results were attributed to the lack of inflow boundary conditions. It was, however, reported that the simulation reasonably predicted the long and narrow flames, as seen in the experimental study. A stratified premixed zone on the rich side of the flame was captured, whereas a non-premixed flame appeared on the lean side.
[124]	LES study of ethanol flames EtF3, EtF6 and EtF8 (Masri et al. 2012) was conducted. The Eulerian/Lagrangian approach was undertaken to model the gaseous and liquid phases. Nicoud's sigma model [94]was used to model turbulent sub-filter stresses (SGS) on two different mesh sizes. Combustion was modelled using the fully adiabatic premixed FGM approach combined with the Artificially Thickened Flame (ATF) method. Progress variable species coefficients were obtained from Chrigui et al. (2013b).	Ethanol with 57 species and 383 reactions Marinov [83]	Studies of the effects of the number of Lagrangian parcels used and the numerical convergence/stability were not performed. The flame length and width for the three flames were reasonably predicted. The gas-phase properties and the droplet velocities were better predicted with increased grid refinement, whereas very little change was noticed for the Sauter Mean Diameter and droplet volume flux. For the EtF3, EtF6 and EtF8 cases, the mean particle velocities compared reasonably well with experimental data. For the EtF8 case, some mismatch was found at far downstream locations. The authors suggested that this could be related to the misprediction of gas-phase velocity associated with issues in turbulence modelling and inflow boundary conditions.
[30] / [31]	Three ethanol flame cases (known as ETF3, ETF6 and ETF7) were simulated using LES to investigate how the structure of dilute sprays is affected by increased turbulence and spray loading. Sensitivity studies relating to the mass fraction of the pre-vaporised fuel at the jet exit plane were performed. A methodology to match the experimental inflow spray data was evaluated. But studies on defining the number of initial droplets parcels used were not performed. Combustion was modelled using ANSYS® Fluent®, and the FGM table is non-adiabatic; however, the effects of heat gain/loss on the species mass fraction were neglected; the chemical reactor is fully non-premixed; the progress variables species coefficients were not informed and only CO_2 and CO was applied.	Ethanol with 50 species and 235 reactions (U.C. [141].	Two-way coupling is used between the Eulerian flow, and the Lagrangian tracked particles. Studies of Lagrangian boundary conditions and convergence /stability analysis were not performed. Increased carrier velocity (case ETF2-7) or decreasing liquid fuel injection mass flow rate (cases ETF2-ETF6) yield a leaner flame and a stronger spray-flow interaction. The flame temperature was usually underpredicted with a deviation up to 60 % at the centre line of flame ETF6 and 20 % for ETF7; the peak of temperature values was usually underpredicted up to 13 %. The numerical uncertainties due to discretisation errors, mesh resolution, numerical instabilities and spray and inlet boundary conditions were believed to 'contaminate' the numerical solution. They concluded that a perturbation of 2 % at the inlet boundary condition for fuel vapour strongly affected flame structure and droplets dynamics. The adiabatic combustion model was not considered as part of the uncertainties.

(*continued on next page*)

Table 4 (*continued*)

Study/ Precursor studies	Details: turbulence and combustion models	Fuel & chemistry mechanism	Lagrangian solver and Combustion assessments
[113]	DNS was performed to study the noise produced by an unconfined ethanol turbulent spray flame, EtF3. The simulation results were compared with experimental data from the University of Sydney [41]. The noise was analysed using spectral content, directivity and sound pressure levels. The Eulerian-Lagrangian framework was employed with a two-way coupling.	Ethanol is modelled using a two-step global reaction model with 6 species [150].	The influence of the initial number of computational parcels prescribed and studies on the Lagrangian solver convergence/stability were not investigated. Statistical quantities for the flow field such as droplet velocities, related fluctuation and gas-phase excess temperature were compared satisfactorily with the available experimental data. The similarity between the DNS flame and premixed and non-premixed flames is reported by analysing the spectral content and directivity. Additionally, the study concluded that the disturbed monopole combustion noise sources are dominant due to unsteady heat release rate fluctuations. With increasing distance away from the nozzle exit, a decreasing emission angle with respect to the flame axis was observed and attributed to refraction effects from temperature-dependent gradients in the flame sound speed.
[128]/[131]	LES Eulerian-Lagrangian with two different combustion models, presumed PDF and ATF, were undertaken. Combustion was modelled using the FGM chemistry table built with fully adiabatic freely propagating premixed at constant equivalence ratio flamelets; progress variable species coefficients were empirically tested using different combinations. The presence of evaporating droplets within the flame model was addressed in this study.	Acetone with 89 species and 419 intermediary reactions Pichon et al. [112].	The influence of the initial number of computational parcels used and studies on Lagrangian solver convergence/stability was not investigated. Both models reproduced the main features of turbulent spray flows well; agreement with experimental data was considered reasonable; the deterministic formalism of the ATF method was more efficient than using the presumed PDF approach. Validation of the combustion model was not performed.
[65]	LES model was used to study turbulent spray flames. A conserved scalar form of the Spalding transfer number approach with an evaporative mixing model that is local in mixture fraction space was used. Combustion was modelled using a stochastic Multiple Mapping condition (MMC) approach.	Acetone with 38 species and 224 chemical reactions [145].	Studies of the Lagrangian solver boundary conditions and convergence/stability were not performed. The simulated results for velocity, liquid volume flow rate, and mean temperature were considered to be in good agreement with experimental data.
[49]	A new framework of LES/partially premixed flamelet modelling for two-phase reacting flows was employed. Combustion was modelled using a partially premixed and fully adiabatic flamelet. The progress variable species coefficients were defined based on an arbitrary approximation to hydrocarbon fuel.	Acetone with 83 species and 419 reactions and 83[112].	Studies of the spray boundary conditions and the Lagrangian solver convergence/stability were not investigated. The partially premixed flamelet method captures the regime transitions satisfactorily. The study found that even with small volumetric distributions, the chemical structures of premixed parts were responsible for changes in the spray evaporation and downstream diffusion reaction.

Computational modelling.

Fourthly, there are fundamental issues regarding the combustion models applied. In fact, for most of the studies reviewed, spray combustion was modelled using tabulated chemistry flamelets, especially the FGM approach. However, the flamelet tables were mainly adiabatic and generated from pure non-premixed chemical reactors. This approach, whilst convenient, is inappropriate for spray combustion because spray flames burn in multi-modes (premixed and non-premixed), and there is heat transfer (evaporation cooling) between the flame and the liquid droplets; thus, requiring the inclusion of non-adiabatic effects in the thermo-chemical tables. Therefore, users of the FGM approach for multiphase spray-flames could not rule out the causes of failures in their combustion outcomes, and most importantly, the limitations underpinning the usage of the FGM have not been analyzed thoroughly.

Fifth, for most of the studies investigated herein, there is a systematic lack of numerical flame validation, and the limitations of the combustion models (including the FGM) are still unknown. This is because the validation of swirl-spray-combustion requires, in the first place, a systematic validation campaign for each individual process starting from non-reacting swirl aerodynamics, the Lagrangian spray modelling, combustion sub-models, and finally, the entire coupled swirl-spray-combustion flame. However, the coupled swirl-spray-combustion analyses require a detailed assessment of the flame turbulence-chemistry interaction (known as a flame regime) based on the Damköhler analysis. This assessment allows identifying limitations in the combustion models that might be associated with issues coming from the chemical time scale predicted from their thermo-chemical table and the effects of turbulent mixing generated from the highly swirling turbulent flow.

Finally, in addition to the five previous points above, a detailed experimental assessment of the flame mode and structure to rule out whether a flame is predominately releasing heat in a non-premixed or premixed mode would be required because it can help modellers in selecting better chemical reactors for spray flame simulations; for instance, most of the thermo-chemical tables in the studies presented in section Computational modelling were generated using pure non-premixed reactors.

Closure remarks

In this review article a systematic compilation and evaluation of laboratory-scale spray-burners databases and results from CFD modelling of spray combustion were presented. A direct correlation between the effectiveness of the burner's dataset and the outcomes achieved from CFD numerical simulations was established. This was investigated to identify the main research gaps in spray combustion modelling and to identify suitable burner databases for numerical modelling development. The main causes of CFD deficiencies and inaccuracies were mostly associated with the inappropriate establishment of numerical inflow boundary conditions (swirl and spray) and inefficient combustion modelling approaches. Laboratory-scale burners which are enclosed with a pressure atomiser and swirling motion can better resemble

Table 4
-2. Summary of computational studies for burners in Table 2-1 and Table 2-2.

Burner Platform/ Study	Turbulence/ combustion/ Software	Boundary conditions. (inflow for non-reacting/ Spray)	Combustion assessments
Imperial College Swirl-Stabilised Axisymmetric /[54–55,57]	LES-*pdf* using the Smagorinsky model. SGS fluctuations were accounted for in the scalars describing the reaction. BOFFIN-LES[54].	Swirler is not included. Inflow condition was generated using adjusted uniform profiles of axial and swirl velocity based on the total flow rate of air.	Two flame conditions were investigated: flames A (stable) and B (approaching blowout). Jet-A was represented using a reduced 7-species chemistry mechanism as in Jones and Tyliszczak [56].
		The spray was defined using a hollow cone (70-80°), with a prescribed fuel flow rate and droplets size modelled based on a Rosin-Rammler distribution. The number of the droplets parcels injected was not presented.	Since the flame was sensitive to the size of the droplets, parametric studies were performed based on changes in the Rosin-Rammler distribution. Species mass fractions were quantitatively analysed as well as flame temperature and the three velocity components. Generally, mean values agreed with experiments, while rms values tended to show significant discrepancies. Failures in computing species concentration were attributed to the reduced chemistry mechanism.
UC Irvine burner[1] / [117–120]	RANS standard k-ε model. A single-step global reaction mechanism was used for *n*-heptane. Turbulence-chemistry interaction was solved with Monte Carlo PDF approach for species and enthalpy. LSPRAY is the Lagrangian phase solver. Domain is 2-D axisymmetric. CFD solver CORSAIR from Pratt and Whitney's Raju [116].	The bulk temperature and velocity were set at the inlet. No further information on turbulence initialisation was provided. The spray was set based on 124 different droplet groups with the fuel flow rate as in the experimental data. The droplets size distribution is in the range of 0–140 μm. The number of droplet parcels was not presented; Lagrangian solver was not validated.	Reacting spray without swirl was compared using both PDF and non-PDF approaches. The PDF approach predicted the dual nature of the spray-flame (diffusion-flame) which was predominant in the domain and some premixed behaviour. Temperature prediction was substantially sensitive to the assumed shaped of the PDF.
	The gas-phase was solved using a	Inlet boundaries started at the first	The effects of particle

Table 4 (*continued*)

Burner Platform/ Study	Turbulence/ combustion/ Software	Boundary conditions. (inflow for non-reacting/ Spray)	Combustion assessments
Yale – Karpetis Spray Burner[2]/ [8] [3]	joint Mass Density Function (MDF). Turbulence is considered by means of a Second-order Momentum Closure.	measurement station at 1.27 mm downstream of the injector. The gas mass flow rate and mean temperature are specified. Inlet dissipation profile was specified. The mixture fraction was imposed homogeneously over all the inlet boundaries.	vaporisation and turbulence interaction were investigated.
	An adiabatic flamelet lookup table was constructed using CHEM1D and FLAME software. Partially premixed effects were not considered.	The spray was set using 9 droplet size classes and a fixed mass flow rate. All droplets have the same temperature and velocity at the inlet. The number of computational parcels selected and their impact on the Lagrangian solver were not investigated.	Computations of the spray flame were improved by reducing drag coefficients and heat and mass transfer for the droplets modelling.
	The Lagrangian equations of the Spray/dispersed phase were solved using the joint-one-point MDF solved using a Monte Carlo method. Two-way coupling effects were accounted for. The domain was solved in 2-D using an in-house Hybrid Lagrangian-Lagrangian solver.		Although the gas axial velocity was well-predicted, the radial velocity is still under-predicted, and it was associated with deficiencies in the vaporisation model, inflow boundary conditions and uncertainties in the experimental data. Mean and RMS of temperature were under-predicted in the peak and spatial locations when compared against the experimental data.
NIST Benchmark Spray Combustion Database[4]/ Zhu et al. [156][5]	RANS standard k-ε model was used for the gas-phase. The domain was 2D axisymmetric and solved using an Eulerian-Lagrangian solved using ANSYS Fluent. A Lagrangian formulation represented the liquid-phase.	The Swirler/ exhaust channel was not included in the domain. The profiles of mean velocities were extrapolated from the downstream location at z = 1.4 mm to the inlet at z = 0 mm. The swirl velocity temperature and mass flow rates were imposed at the inlet. Spray atomisation was performed using the LISA break-up	The spray boundary conditions (exit injector diameter, dispersion angle and mean droplet SMD size) influenced the spray spread, hence changing droplet spread and velocities predictions; these were considered the primary source of uncertainties.

(*continued on next page*)

Table 4 (*continued*)

Burner Platform/ Study	Turbulence/ combustion/ Software	Boundary conditions. (inflow for non-reacting/ Spray)	Combustion assessments
		model. Breakup parameters were estimated from published correlations, the atomiser pressure and exit diameter. Trial-and-error was applied to estimate and optimise spray parameters with the experimental data.	
	Combustion was modelled using ANSYS® Fluent® and the non-adiabatic Steady Laminar Flamelet (SLF); however, the effects of heat gain/loss on the species mass fraction were neglected; the chemical reactor is non-premixed; the choice of the progress variables species coefficients was not explained.		Quantitative analysis is presented and accompanied by possible reasons for discrepancies. The authors also argued for the necessity of near nozzle spray measurements hence improving the accuracy of the CFD boundary conditions. Overall, since temperature measurements in the flame were not available, a direct comparison with CFD was not performed. Therefore, an analysis of the accuracy of the flamelet approach was not assessed.
CNRS Orleans burner/ Sacomano et al. [129]	The gas-phase (Eulerian) was solved using LES with the Dynamics Smagorinsky model.	Constant and uniform velocity profiles were set at the inlet of the extruded duct. The pilot flame was surrounded by coflow air at constant inlet velocity. LES inflow initialisation strategy was not investigated.	Three different equivalence ratios were tested for parametric flame structure analysis. The flame was essentially burning in a premixed mode.
	Turbulence-chemistry interaction was modelled using the Artificially Thickened Flame (ATF) coupled with the Flamelet Generated Manifold (FGM) combustion model.	At the boundary of injection, the droplets were already diluted; hence no breakup models were required. The mixture fraction of the pre-vaporised fuel was set at the inlet. Further details on boundary conditions are found in Sacomano et al. [130] as implemented in the FATEST3D CFD	Four classes of droplet size distributions were assessed at the droplet injection boundary for validation purposes. But the choice of the impact of the number of droplets injected was not investigated.

Table 4 (*continued*)

Burner Platform/ Study	Turbulence/ combustion/ Software	Boundary conditions. (inflow for non-reacting/ Spray)	Combustion assessments
		solver. The pilot flame was associated with a fully burned flamelet.	
	Eulerian-Lagrangian scheme via a two-way coupling was used. Tabulated chemistry was generated using premixed and fully adiabatic flamelets at a constant equivalence ratio.		Using the artificial thickening approach, a series of modelling issues were discussed, e.g., the effects of mass imbalance and evaporation issues on the dispersed phase. Detailed analysis of the effects of sub-grid scale flame wrinkling models on the flame structure was presented. Even though not pursued in this present study, the necessity of the development and inclusion of heat losses and detailed chemistry on the FGM table was acknowledged to improve flame and evaporating-droplets interactions accuracy.
Heidelberg Burner / Düwel et al. [27]	The gas-phase (Eulerian) was solved using a standard RANS k-ε model. Combustion was modelled using a spray flamelet library as presented in Hollmann and Gutheil [47] with a Stochastic Separated Flow (SSF) approach. A steady and two-dimensional (axisymmetric) Eulerian-Lagrangian scheme was used. The influence of turbulence on droplets was accounted for.	Gas-phase inlet velocity was estimated from the total flux of the air coflow. Inflow turbulence properties were not mentioned. The spray was diluted and represented by a finite number of parcels estimated from the first measurement station. The temperature of the droplets was set as 45 °C for all parcels. The Lagrangian solver was not validated.	The spray flamelet library was generated using detailed transport and chemical reactions, thus allowing for detailed radical and pollutant analysis.
			For non-reacting cases, predictions for the mean droplet velocity (axial and radial components) were usually 30% higher than those

(*continued on next page*)

Table 4 (*continued*)

Burner Platform/ Study	Turbulence/ combustion/ Software	Boundary conditions. (inflow for non-reacting/ Spray)	Combustion assessments
			from the experiments, thus affecting the prediction of the droplets evaporation rate, with the predicted droplet radii up to 10% off the experimental data. Results were quantitatively assessed using the temperature profile at four different downstream locations. Generally, the results are mismatched in the radial direction. The main sources of uncertainties were related to unknown initial gas flow properties and uncertainties in measurements of the initial droplet size distribution due to a coarse spatial resolution.

[1] This burner has also been investigated by Ge and Gutheil [36] using a 2-D axisymmetric steady-state RANS k-ε for the gas-phase, spray-flamelets and a PDF approach for the mixture fraction. Enthalpy and gas temperature models revealed strongly correlated with the enthalpy and mixture fractions. The results were sensitive to the mixing model constant that largely influences the main gas velocity and temperature results; Hollmann and Gutheil [48,47] also carried out previous simulations.

[2] This flame has also been investigated by Jones et al. [54] using an Eulerian stochastic method for turbulence-chemistry interaction with a Lagrangian formulation. The sub-grid scale (SGS) influence on droplet evaporation and dispersion was stochastically accounted for.

[3] This study is regarded as the first attempt to investigate this flame.

[4] Itoh et al. [52] investigated this flame using an LES Eulerian-Lagrangian approach. Mean profiles of the air inlet velocity were obtained from the experimental data, and the velocity fluctuations at the LES inflow were neglected. Lagrangian-spray inlet boundary conditions were extrapolated from experimental data starting at a location 5 mm downstream of the injector nozzle; there was no information for the number of droplet parcels used Lagrangian solver was not validated. It was argued that including the effects of inlet fluctuations as well as increasing the number of droplets at the inlet would have improved the computed numerical accuracy.

[5] Studies of this flame prior to 2015 are reviewed by Zhu et al. [156]. Numerical results are quantitatively contrasted with previous simulations of Collazo et al. [25].

aeronautical gas turbines because the flame is swirl-stabilised; the same phenomenology does not happen when the burner is non-swirling or stabilised by a pilot flame. In addition, few burners investigated herein have accessible databases with flame measurements of biofuels.

Overall, a preference for the use of flamelets in modelling combustion is observed, together with the use of the Lagrangian framework for spray modelling and the use of steady-state RANS k-ε and LES for turbulence closure. However, six key issues that can lead to numerical uncertainties and difficulties in validation were identified from the numerical studies presented in section Computational modelling. For most of the studies, the discrepancies and mispredictions of the flame structure and gas-phase velocities in the CRZ were related to the lack of appropriate establishment of swirl inflow boundary conditions and issues attributed to inefficient turbulence modelling. The Lagrangian approach with a dispersed liquid phase and the Rosin-Rammler droplets size distribution were predominately applied in spray simulations. However, for most of the studies, there was no investigation of the impact of the initial number of computational droplet parcels on the Lagrangian solver convergence/stability, and validation is still elusive; thus, uncertainties coming from the choice of the number of parcels were not ruled out nor the impact of this on actual flame physics. Several issues regarding combustion modelling were identified. Most of the flamelet tables were generated using fully adiabatic flamelets. Hence, the effects of convective heat transfer (evaporative cooling) and the impact of heat gain/loss on species mass fraction were disregarded. Furthermore, the choice of progress variable species coefficients was usually arbitrarily selected, and no clear consensus on its definition was discussed for biofuels. Despite numerical and experimental evidence that spray flames are partially premixed, the FGM tables were still generated using non-premixed counter diffusion reactors, thus, jeopardising the resolution of a flame in case a premixed region appears. Most of the studies drew attention to the necessity of including heat loss effects within the tables, especially with detailed chemistry as a means of improving the predictability of flame temperature and structure (OH-distribution, lift-off and shape). In addition, Ma and Roekaerts [79] hypothesised the possibility of applying perfectly mixed homogenous igniting reactors to improve the FGM tables for predicting spray combustion. Furthermore, a detailed evaluation of the swirl flame initialisation (forced ignition) process was missing in all numerical studies investigated, and no recommendations on flame initialisation were suggested. Finally, studies to understand and rule out the limitations and sources of uncertainties in the combustion models applied were inconclusive and unexplored mostly because the assessment of the flame mode and the effects of the turbulence-chemistry interactions were neglected. Thus, detailed experimental assessments of the flame mode and structure are required to help modellers in selecting better chemical reactors for spray flame simulations. Improvements in experimental techniques and data characterization must be combined with improved and validated numerical algorithms to advance the knowledge of turbulent spray flames.

Declaration of Competing Interest

The authors declare that they have no known competing financial interests or personal relationships that could have appeared to influence the work reported in this paper.

Acknowledgements

This work has been financially supported by the Centre for Fluid and Complex Systems at Coventry University, and partly by the UGC-UKIERI 2016-17-050 grant.

References

[1] Abramzon B, Sirignano WA. Droplet Vaporization Model for Spray Combustion Calculations. Int J Heat Mass Transf 1989;32(9):1605–18.
[2] Abtahizadeh E, de Goey P, van Oijen J. LES of Delft Jet-in-Hot Coflow Burner to Investigate the Effect of Preferential Diffusion on Autoignition of CH4/H2 Flames. Fuel 2017;191:36–45.
[3] Abtahizadeh E, de Goey P, van Oijen J. Development of a Novel Flamelet-Based Model to Include Preferential Diffusion Effects in Autoignition of CH4/H2 Flames. Combust Flame 2015;162(11):4358–69.

[4] Abtahizadeh SE. Numerical study of mild combustion: from laminar flames to Large Eddy Simulation of turbulent flames with Flamelet Generated Manifolds. Eindhoven: Technische Universiteit Eindhoven; 2014. PhD thesis.
[5] Adachi M, McDonell V, Samuelsen G. Non-Intrusive Measurement of Gaseous Species in Reacting and Non-Reacting Sprays. Combust Sci Technol 1991;75 (4–6):179–94.
[6] Al-Abdeli YM, Masri AR. Review of Laboratory Swirl Burners and Experiments for Model Validation. Exp Therm Fluid Sci 2015;69:178–96.
[7] Beér JM, Chigier NA. Combustion Aerodynamics. London: Applied Science Publishers Ltd; 1972.
[8] Beishuizen NA. PDF modelling and particle-turbulence interaction of turbulent spray flames. Eindhoven: Technische Universiteit Eindhoven; 2014. PhD thesis.
[9] Branley N, Jones WP. Large Eddy Simulation of a Turbulent Non-Premixed Flame. Combust Flame 2001;127(1–2):1914–34.
[10] Brito Lopes AV (2021). *Advanced Modelling of Turbulent Spray Flames in Aero Gas-Turbines with Liquid Bio-Fuels*. PhD thesis. Coventry: Coventry University.
[11] Brito Lopes AV, Emekwuru N. Impact of the number of computational parcels on the prediction of highly swirling spray-flame mode and structure. ProceedIngs of the 10th European Combustion MeetIng – Virtual Edition. 2021. https://www.ecm2021napoli.eu/proceedings/.
[12] Brito Lopes AV, Emekwuru N, Bonello B, Abtahizadeh E. On the Highly Swirling Flow through a Confined Bluff-Body. Phys Fluids 2020;32(5):055105.
[13] Bulzan DL. 'Velocity and drop size measurements in a confined, swirl-stabilized, combustion spray'. In *32nd Joint Propulsion Conference and Exhibit*. held 1-3 July 1996 at Lake Buena, Fl, U.S.A. ed. by American Institute of Aeronautics and Astronautics (1996).
[14] Bulzan DL. Structure of a Swirl-Stabilized Combusting Spray. J Propul Power 1995;11(6):1093–102.
[15] Cabra R, Hamano Y, Chen JY, Dibble RW, Acosta F, and Holve D. ' Ensemble diffraction measurements of spray combustion in a novel vitiated coflow turbulent jet flame burner' [online] (2000) available from < https://ntrs.nasa.gov/api/citations/20000112945/downloads/20000112945.pdf> [03 Aug. 2018].
[16] Cavaliere DE. Blow-Off in Gas Turbine Combustors. Cambridge: University of Cambridge; 2013. PhD thesis.
[17] Cavaliere DE, Kariuki J, Mastorakos E. A Comparison of the Blow-Off Behaviour of Swirl-Stabilized Premixed, Non-Premixed and Spray Flames. Flow, Turbulence Combust 2013;91(2):347–72.
[18] Cheng X, Chen L, Yan F. Study of the Characteristic of Diesel Spray Combustion and Soot Formation using Laser-Induced Incandescence (LII). J Energy Inst 2014; 87(4):383–92.
[19] Chong CT, Hochgreb S. Spray Flame Study using a Model Gas Turbine Swirl Burner. Appl Mech Mater 2013;316–317:17–22.
[20] Chong CT, Hochgreb S. Spray Combustion Characteristics of Palm Biodiesel. Combust Sci Technol 2012;184(7–8):1093–107.
[21] Chrigui M, Gounder J, Sadiki A, Janicka J, Masri AR. Acetone Droplet Behavior in Reacting and Non-Reacting Turbulent Flow. Flow, Turbulence Combust 2013;90 (2):419–47.
[22] Chrigui M, Masri AR, Sadiki A, Janicka J. Large Eddy Simulation of a Polydisperse Ethanol Spray Flame. Flow, Turbulence Combust 2013;90(4):813–32.
[23] Chrigui M, Gounder J, Sadiki A, Masri AR, Janicka J. Partially premixed reacting acetone spray using LES and FGM tabulated chemistry. Combust Flame 2012;159 (8):2718–41.
[24] Chrigui M, Sadiki A, Gounder J, Masri A. Numerical and Experimental Study of Polydispersed Acetone Spray Dispersion and Evaporation in Turbulent Flow. In: ASME Turbo Expo: Turbine Technical Conference and Exposition, GT2011-46301; 2011. p. 1055–64.
[25] Collazo J, Porteiro J, Patiño D, Miguez JL, Granada E, Moran J. Simulation and Experimental Validation of a Methanol Burner. Fuel 2009;88(2):326–34.
[26] Domingo P, Vervisch L, Réveillon J. DNS Analysis of Partially Premixed Combustion in Spray and Gaseous Turbulent Flame-Bases Stabilized in Hot Air. Combust Flame 2005;140(3):172–95.
[27] Düwel I, Ge H, Kronemayer H, Dibble R, Gutheil E, Schulz C, et al. Experimental and Numerical Characterization of a Turbulent Spray Flame. Proc Combust Inst 2007;31(2):2247–55.
[28] Edwards C, Rudoff R. Structure of a Swirl-Stabilized Spray Flame by Imaging, Laser Doppler Velocimetry, and Phase Doppler Anemometry. Symp (Int) Combust 1991;23(1):1353–9.
[29] Eckel G, Grohmann J, Cantu L, Slavinskaya N, Kathrotia T, Rachner M, et al. LES of a Swirl-Stabilized Kerosene Spray Flame with a Multi-Component Vaporization Model and Detailed Chemistry. Combust Flame 2019;207:134–52.
[30] El-Asrag H, Braun M, Masri AR. Large eddy simulations of partially premixed ethanol dilute spray flames using the flamelet generated manifold mode. Combust Theor Model 2016;20(4):567–91.
[31] El-Asrag HA, Braun M. Effect of turbulence non-isotropy modeling on spray dynamics for an evaporating Acetone spray jet. Int J Multiph Flow 2015;68: 100–20.
[32] Ertesvåg IS, Magnussen BF. The Eddy Dissipation Turbulence Energy Cascade Model. Combust Sci Technol 2000;159(1):213–35.
[33] Ertesvåg IS. Analysis of some Recently Proposed Modifications to the Eddy Dissipation Concept (EDC). Combust Sci Technol 2020;192(6):1108–36.
[34] Fiorina B, Van CN. Joined comparative study of the CORIA Rouen Spray Burner Simulation instructions [online]. (2019) available from <http://www.tcs-workshop.org/> [08 Mar. 2020].
[35] Ge W, Sankaran R, Chen JH. Development of a CPU/GPU Portable Software Library for Lagrangian-Eulerian Simulations of Liquid Sprays. Int J Multiph Flow 2020;128:103293.
[36] Ge H, Gutheil E. Simulation of a Turbulent Spray Flame using Coupled PDF Gas Phase and Spray Flamelet Modeling. Combust Flame 2008;153(1–2):173–85.
[37] Germano M, Piomelli U, Moin P, Cabot WH. A Dynamic subgrid-scale Eddy Viscosity Model. Phys Fluids A 1991;3(7):1760–5.
[38] Giusti A, Kotzagianni M, Mastorakos E. LES/CMC Simulations of Swirl-Stabilised Ethanol Spray Flames Approaching Blow-Off. Flow, Turbulence Combust 2016;97 (4):1165–84.
[39] Giusti A, Mastorakos E. Detailed Chemistry LES/CMC Simulation of a Swirling Ethanol Spray Flame Approaching Blow-Off. Proc Combust Inst 2017;36(2): 2625–32.
[40] Giusti A, Mastorakos E. Turbulent Combustion Modelling and Experiments: Recent Trends and Developments. Flow, Turbulence Combust 2019;103(4): 847–69.
[41] Gounder JD, Kourmatzis A, Masri AR. Turbulent Piloted Dilute Spray Flames: Flow Fields and Droplet Dynamics. Combust Flame 2012;159(11):3372–97.
[42] Grohmann J, O'Loughlin W, Meier W, Aigner M. Comparison of the Combustion Characteristics of Liquid Single-Component Fuels in a Gas Turbine Model Combustor. ASME Turbo Expo 2016: Turbomachinery Technical Conference and Exposition 49750, V04AT04A010. American Society of Mechanical Engineers; 2016.
[43] Grohmann J, Rauch B, Kathrotia T, Meier W, Aigner M. Influence of Single-Component Fuels on Gas-Turbine Model Combustor Lean Blowout. J Propul Power 2018;34(1):97–107.
[44] Hardalupas Y, Taylor AMKP, Whitelaw JH, Weinberg FJ. 'Velocity and Size Characteristics of Liquid-Fuelled Flames Stabilized by a Swirl Burner'. *Proceedings of the Royal Society of London. A. Mathematical and Physical Sciences* 428 (1990), 129-155.
[45] Heye C, Raman V, Masri AR. LES/probability density function approach for the simulation of an ethanol spray flame. Proc Combust Inst 2013;34(1):1633–41.
[46] Hochgreb S. Mind the gap: Turbulent combustion model validation and future needs. Proc Combust Inst 2019;37(2):2091–107.
[47] Hollmann C, Gutheil E. Diffusion Flames Based on a Laminar Spray Flame Library. Combust Sci Technol 1998;135(1–6):175–92.
[48] Hollmann C, Gutheil E. Modeling of Turbulent Spray Diffusion Flames Including Detailed Chemistry. Symp (Int) Combust 1996;26(1):1731–8.
[49] Hu Y, Kurose R. Partially premixed flamelet in LES of acetone spray flames. Proc Combust Inst 2019;37(3):3327–34.
[50] Ihme M, Pitsch H. Modeling of Radiation and Nitric Oxide Formation in Turbulent Nonpremixed Flames using a flamelet/progress Variable Formulation. Phys Fluids 2008;20(5):055110.
[51] IPCC (1999) *Aviation and the Global Atmosphere* [online] available from <https://www.ipcc.ch/report/aviation-and-the-global-atmosphere-2/> [13 Jun. 2019].
[52] Itoh Y, Taniguchi N, Kobayashi T, Tominaga T. Large Eddy Simulation of spray combustion in swirling flows. In *ASME/JSME 4th Joint Fluids Summer Engineering Conference* FEDSM2003-45383. (2003), 1505-1510.
[53] Jenny P, Roekaerts D, Beishuizen N. Modeling of turbulent dilute spray combustion. Prog Energy Combust Sci 2012;38(6):846–87.
[54] Jones WP, Lyra S, Navarro-Martinez S. Numerical Investigation of Swirling Kerosene Spray Flames using Large Eddy Simulation. Combust Flame 2012;159 (4):1539–61.
[55] Jones WP, Lyra S, Navarro-Martinez S. Large Eddy Simulation of a Swirl Stabilized Spray Flame. Proc Combust Inst 2011;33(2):2153–60.
[56] Jones WP, Tyliszczak A. Large Eddy Simulation of Spark Ignition in a Gas Turbine Combustor. Flow, Turbulence Combust 2010;85(3):711–34.
[57] Jones WP, Sheen D. A Probability Density Function Method for Modelling Liquid Fuel Sprays. Flow, Turbulence Combust 2000;63(1):379–94.
[58] Kariuki J, Mastorakos E. Experimental Investigation of Turbulent Flames in Uniform Dispersions of Ethanol Droplets. Combust Flame 2017;179:95–116.
[59] Karpetis AN, Gomez A. An Experimental Study of Well-Defined Turbulent Nonpremixed Spray Flames. Combust Flame 2000;121(1–2):1–23.
[60] Karpetis AN, Gomez A. Self-Similarity, Momentum Scaling and Reynolds Stress in Non-Premixed Turbulent Spray Flames. J Fluid Mech 1999;397:231–58.
[61] Karpetis AN, Gomez A. An Experimental Investigation of Non-Premixed Turbulent Spray Flames and their Self-Similar Behavior. Symp (Int) Combust 1998;27(2):2001–8.
[62] Karpetis AN, Gomez A. Temperature Measurements in Spray Flames by Spontaneous Raman Scattering. Opt Lett 1996;21(10):704–6.
[63] Kärrholm FP. Numerical Modelling of Diesel Spray Injection, Turbulence Interaction and Combustion. Gothenburg: Chalmers University of Technology; 2018. PhD thesis.
[64] Kathrotia T. Reaction Kinetics modelling of OH*, CH*, and C2* chemiluminescence. Heidelberg: Ruprecht-Karls-Universitat; 2015. PhD thesis.
[65] Khan N, Cleary MJ, Stein OT, Kronenburg A. A two-phase MMC–LES model for turbulent spray flames. Combust Flame 2018;193:424–39.
[66] Khalil AEE, Brooks JM, Gupta AK. Impact of Confinement on Flowfield of Swirl Flow Burners. Fuel 2016;184:1–9.
[67] Klimenko AY, Bilger RW. Conditional Moment Closure for Turbulent Combustion. Prog Energy Combust Sci 1999;25(6):595–687.
[68] Kronenburg A, Kostka M. Modeling Extinction and Reignition in Turbulent Flames. Combust Flame 2005;143(4):342–56.
[69] Kuo KKY, Acharya R. Fundamentals of turbulent and multiphase combustion. Hoboken: John Wiley & Sons; 2012.
[70] Letty C, Mastorakos E, Masri AR, Juddoo M, O'Loughlin W. Structure of Igniting Ethanol and n-Heptane Spray Flames with and without Swirl. Exp Therm Fluid Sci 2012;43:47–54.

[71] Lewandowski MT, Li Z, Parente A, Pozorski J. Generalised Eddy Dissipation Concept for MILD Combustion Regime at Low Local Reynolds and Damköhler Numbers. Part 2: Validation of the Model. Fuel 2020;278:117773.
[72] Lilley DG. Swirl Flows in Combustion: A Review. AIAA J 1977;15(8):1063–78.
[73] Luo K, Pitsch H, Pai MG, Desjardins O. Direct Numerical Simulations and Analysis of Three-Dimensional n-Heptane Spray Flames in a Model Swirl Combustor. Proc Combust Inst 2011;33(2):2143–52.
[74] Lefebvre AH. Gas Turbine Combustion. London: Taylor & Francis; 1999.
[75] Lefebvre AH, Ballal DR. Gas Turbine Combustion: Alternative Fuels and Emissions. Boca Raton: CRC Press; 2010.
[76] Lehnhäuser T, Schäfer M. Improved Linear Interpolation Practice for Finite-Volume Schemes on Complex Grids. Int J Numer Meth Fluids 2002;38(7):625–45.
[77] Lieuwen TC. Unsteady Combustor Physics. New York: Cambridge University Press; 2012.
[78] Ma L. Computational Modeling of Turbulent Spray Combustion. Delft: Delft University of technology; 2016. PhD thesis.
[79] Ma L, Roekaerts D. Modeling of Spray Jet Flame Under MILD Condition with Non-Adiabatic FGM and a New Conditional Droplet Injection Model. Combust Flame 2016;165:402–23.
[80] Ma L, Naud B, Roekaerts D. Transported PDF Modeling of Ethanol Spray in Hot-Diluted Coflow Flame. Flow, Turbulence Combust 2016;96(2):469–502.
[81] Ma L, Zhu S, Tummers M, Van Der Meer T, Roekaerts D. Numerical Investigation of Ethanol Spray-in-Hot-Coflow Flame using Steady Flamelet Model. Eighth Mediterranean Combustion Symposium. held 8–13 September at Cesme. 2013.
[82] Maas U, Pope SB. Simplifying Chemical Kinetics: Intrinsic Low-Dimensional Manifolds in Composition Space. Combust Flame 1992;88(3–4):239–64.
[83] Marinov NM. A Detailed Chemical Kinetic Model for High Temperature Ethanol Oxidation. Int J Chem Kinet 1999;31(2–3):183–220.
[84] Masri AR, Gounder JD. *'Details and Complexities of Boundary Conditions in Turbulent Piloted Dilute Spray Jets and Flames'*. In: Merci B., Roekaerts D., Sadiki A. (eds.) Experiments and Numerical Simulations of Diluted Spray Turbulent Combustion. ERCOFTAC Series, 17. Dordrecht: Springer Netherlands (2011).
[85] Masri AR, Gounder JD. Turbulent Spray Flames of Acetone and Ethanol Approaching Extinction. Combust Sci Technol 2010;182(4–6):702–15.
[86] McDonell VG, Adachi M, Samuelsen GS. Structure of Reacting and Non-Reacting Swirling Air-Assisted Sprays. Combust Sci Technol 1992;82(1–6):225–48.
[87] McDonell VG, Samuelsen GS. Application of Laser Interferometry to the Study of Droplet' Gas Phase Interaction and Behavior in Liquid Spray Combustion Systems. Combust Sci Technol 1990;74(1–6):343–59.
[88] McDonell VG, Samuelsen GS. Structure of vaporizing pressure atomized sprays. Atomization Sprays 1993;3(3):321–64.
[89] McDonell VG, Samuelsen GS. An Experimental Data Base for the Computational Fluid Dynamics of Reacting and Nonreacting Methanol Sprays. J Fluids Eng 1995;117(1):145–53.
[90] Melton LA. Soot Diagnostics Based on Laser Heating. Appl Opt 1984;23(13):2201–8.
[91] Mohd Yasin MF, Cant RS, Chong CT, Hochgreb S. Discrete Multicomponent Model for Biodiesel Spray Combustion Simulation. Fuel 2014;126:44–54.
[92] Mohaddes D, Xie W, Ihme M. Analysis of Low-Temperature Chemistry in a Turbulent Swirling Spray Flame Near Lean Blow-Out. Proc Combust Inst 2021;38(2):3435–43.
[93] Nau P, Yin Z, Lammel O, Meier W. Wall Temperature Measurements in Gas Turbine Combustors with Thermographic Phosphors. J Eng Gas Turbines Power 2018;141(4):041021.
[94] Nicoud F, Toda HB, Cabrit O, Bose S, Lee J. Using Singular Values to Build a Subgrid-Scale Model for Large Eddy Simulations. Phys Fluids 2011;23(8):085106.
[95] Oijen JAV, Donini A, Bastiaans RJM, ten Thije Boonkkamp JHM, de Goey LPH. State-of-the-Art in Premixed Combustion Modeling using Flamelet Generated Manifolds. Prog Energy Combust Sci 2016;57:30–74.
[96] Oijen JAV, Bastiaans RJM, de Goey LPH. Low-Dimensional Manifolds in Direct Numerical Simulations of Premixed Turbulent Flames. Proc Combust Inst 2007;31(1):1377–84.
[97] Oijen JAV, Groot GRA, Bastiaans RJM, de Goey LPH. A Flamelet Analysis of the Burning Velocity of Premixed Turbulent Expanding Flames. Proc Combust Inst 2005;30(1):657–64.
[98] Oijen JAV, de Goey LPH. A Numerical Study of Confined Triple Flames using a Flamelet-Generated Manifold. Combust Theor Model 2004;8(1):141–63.
[99] Oijen JAV, de Goey LPH. Modelling of Premixed Counterflow Flames using the Flamelet-Generated Manifold Method. Combust Theor Model 2002;6(3):463–78.
[100] Oijen JAV. Flamelet-generated manifolds: development and application to premixed laminar flames. Eindhoven: Eindhoven University Press; 2002.
[101] Oijen JAV, Lammers FA, de Goey LPH. Modeling of Complex Premixed Burner Systems by using Flamelet-Generated Manifolds. Combust Flame 2001;127(3):2124–34.
[102] Oijen JAV, Goey LPHD. Modelling of Premixed Laminar Flames using Flamelet-Generated Manifolds. Combust Sci Technol 2000;161(1):113–37.
[103] Pascaud S, Boileau M, Cuenot B, Poinsot T. Large Eddy Simulation of Turbulent Spray Combustion in Aeronautical Gas Turbines. In: ECCOMAS Thematic Conference on Computational Combustion; 2005. p. 149–67.
[104] Paulhiac D, Cuenot B, Riber E, Esclapez L, Richard S. Analysis of the Spray Flame Structure in a Lab-Scale Burner using Large Eddy Simulation and Discrete Particle Simulation. Combust Flame 2020;212:25–38.
[105] Pera C, Réveillon J, Vervisch L, Domingo P. Modeling Subgrid Scale Mixture Fraction Variance in LES of Evaporating Spray. Combust Flame 2006;146(4):635–48.
[106] Pope SB. Turbulent Flows. Cambridge: Cambridge University Press; 2000.
[107] Peters N. Turbulent Combustion. Cambridge: Cambridge University Press; 2000.
[108] Peters N. The Turbulent Burning Velocity for Large-Scale and Small-Scale Turbulence. J Fluid Mech 1999;384:107–32.
[109] Peters N. Laminar Flamelet Concepts in Turbulent Combustion. Symp (Int) Combust 1988;21(1):1231–50.
[110] Peters N. Laminar Diffusion Flamelet Models in Non-Premixed Turbulent Combustion. Prog Energy Combust Sci 1984;10(3):319–39.
[111] Pichard C, Michou Y, Chauveau C, Gökalp L. Average Droplet Vaporization Rates in Partially Prevaporized Turbulent Spray Flames. Proc Combust Inst 2002;29(1):527–33.
[112] Pichon S, Black G, Chaumeix N, Yahyaoui M, Simmie JM, Curran HJ, et al. The Combustion Chemistry of a Fuel Tracer: Measured Flame Speeds and Ignition Delays and a Detailed Chemical Kinetic Model for the Oxidation of Acetone. Combust Flame 2009;156(2):494–504.
[113] Pillai AL, Kurose R. Numerical investigation of combustion noise in an open turbulent spray flame. Appl Acoust 2018;133:16–27.
[114] Poinsot T. Prediction and Control of Combustion Instabilities in Real Engines. Proc Combust Inst 2017;36:1–28.
[115] Poinsot T, Veynante D. Theoretical and Numerical Combustion. Philadelphia: RT Edwards Inc; 2005.
[116] Raju MS. *LSPRAY-V: A Lagrangian Spray Module*. NASA/CR-2015-218918, NASA Glenn Research Center, Cleveland, Ohio (2015).
[117] Raju M, Bulzan D. Current Status of Superheat Spray Modeling With NCC. In *48th AIAA/ASME/SAE/ASEE Joint Propulsion Conference & Exhibit.* held 30 July to 01 August 2012 at Atlanta, Georgia, U.S.A. ed. by American Institute of Aeronautics and Astronautics (2012).
[118] Raju MS. LSPRAY-III: A Lagrangian Spray Module, NASA/CR–2008-215290. Cleveland, Ohio: NASA Glenn Research Center; 2008.
[119] Raju MS. EUPDF-II: An Eulerian Joint Monte Carlo PDF Module, NASA/CR–2004-213073. Cleveland, Ohio: NASA Glenn Research Center; 2004.
[120] Raju MS. Application of Scalar Monte Carlo Probability Density Function Method for Turbulent Spray Flames. Numer Heat Transfer, Part A: Appl 1996;30(8):753–77.
[121] Rauch B, Calabria R, Chiariello F, Le Clercq P, Massoli P, Rachner M. Accurate Analysis of Multicomponent Fuel Spray Evaporation in Turbulent Flow. Exp Fluids 2012;52(4):935–48.
[122] Renou, B.; Cabot, G.; Santiago, J.M.; Verdier, A. (2017) Description of the experimental facility and list of data. *6th Workshop on the Turbulent Calculations of Sprays*. Available from <http://www.tcs-workshop.org/> [13 Feb. 2019].
[123] Réveillon J, Vervisch L. Analysis of Weakly Turbulent Dilute-Spray Flames and Spray Combustion Regimes. J Fluid Mech 2005;537:317–47.
[124] Rittler A, Proch F, Kempf AM. LES of the Sydney piloted spray flame series with the PFGM/ATF approach and different sub-filter models. Combust Flame 2015;162(4):1575–98.
[125] Rodrigues HC. Spray Combustion in Moderate and Intense Low-Oxygen Conditions: An Experimental Study. Delft: Delft University of Technology; 2015. PhD thesis.
[126] Rodrigues HC, Tummers MJ, van Veen EH, Roekaerts DJEM. Effects of Coflow Temperature and Composition on Ethanol Spray Flames in Hot-Diluted Coflow. Int J Heat Fluid Flow 2015;51:309–23.
[127] Rodrigues HC, Tummers MJ, van Veen EH, Roekaerts DJEM. Spray Flame Structure in Conventional and Hot-Diluted Combustion Regime. Combust Flame 2015;162(3):759–73.
[128] Sacomano Filho FL, Kadavelil J, Staufer M, Sadiki A, Janicka J. Analysis of LES-based combustion models applied to an acetone turbulent spray flame. Combust Sci Technol 2019;191(1):54–67.
[129] Sacomano Filho FL, Kuenne G, Chrigui M, Sadiki A, Janicka J. A consistent Artificially Thickened Flame approach for spray combustion using LES and the FGM chemistry reduction method: Validation in Lean Partially Pre-vaporized flames. Combust Flames 2017;184:68–89.
[130] Sacomano Filho FL, Chrigui M, Sadiki A, Janicka J. Les-Based Numerical Analysis of Droplet Vaporization Process in Lean Partially Premixed Turbulent Spray Flames. Combust Sci Technol 2014;186(4–5):435–52.
[131] Sacomano Filho FL, Fukumasu NK, Krieger GC. Numerical simulation of an ethanol turbulent spray flame with RANS and diffusion combustion model. J Braz Soc Mech Sci Eng 2013;35(3):189–98.
[132] Sadiki A, Chrigui M, Janicka J, Maneshkarimi M. Modeling and Simulation of Effects of Turbulence on Vaporization, Mixing and Combustion of Liquid-Fuel Sprays. Flow, Turbulence Combust 2005;75(1):105–30.
[133] Sánchez AL, Urzay J, Liñán A. The Role of Separation of Scales in the Description of Spray Combustion. Proc Combust Inst 2015;35(2):1549–77.
[134] Schönfeld T, Rudgyard M. Steady and Unsteady Flow Simulations using the Hybrid Flow Solver AVBP. AIAA J 1999;37(11):1378–85.
[135] Shum-Kivan F, Marrero Santiago J, Verdier A, Riber E, Renou B, Cabot G, et al. Experimental and Numerical Analysis of a Turbulent Spray Flame Structure. Proc Combust Inst 2017;36(2):2567–75.
[136] Sheen D. *Swirl-stabilised turbulent spray flames in an axisymmetric model combustor*. PhD thesis. London: Imperial College London (1993).
[137] Slotnick J, Khodadoust A, Alonso J, Darmofal D, Gropp W, Lurie E, et al. *CFD Vision 2030 Study: A Path to Revolutionary Computational Aerosciences*, NASA/CR–2014-218178. Hampton, Virginia: NASA Langley Research Center; 2014.
[138] Sidey JAM, Giusti A, Benie P, Mastorakos E *The Swirl Flames Data Repository* (2017) [online] available from <http://swirl-flame.eng.cam.ac.uk> [25 Mar. 2018].
[139] Turns SR. An Introduction to Combustion: Concepts and Applications. Mechanical Engineering Series. New York: McGraw-Hill Companies; 2000.

[140] Tyliszczak A, Cavaliere DE, Mastorakos E. LES/CMC of Blow-Off in a Liquid Fueled Swirl Burner. Flow, Turbulence Combust 2014;92(1):237–67.
[141] U. C. San Diego (2011) Chemical-kinetic mechanisms for combustion applications. San Diego mechanism web page, Mechanical and aerospace engineering (Combustion Research), University of California at San Diego [online] available from ≤http://combustion.ucsd.edu≥ [25 Mar. 2018].
[142] Ukai S, Kronenburg A, Stein OT. Certain Aspects of Conditional Moment Closure for Spray Flame Modelling. In: High Performance Computing in Science and Engineering. Cham: Springer International Publishing; 2015. p. 335–50.
[143] Ukai S, Kronenburg A, Stein OT. Large eddy simulation of dilute acetone spray flames using CMC coupled with tabulated chemistry. Proc Combust Inst 2015;35(2):1667–74.
[144] Ukai S, Kronenburg A, Stein OT. Simulation of Dilute Acetone Spray Flames with LES-CMC Using Two Conditional Moments. Flow, Turbulence Combust 2014;93(3):405–23.
[145] Ukai S, Kronenburg A, Stein OT. LES-CMC of a dilute acetone spray flame. Proc Combust Inst 2013;34(1):1643–50.
[146] U.S Secretary of Commerce (2018) 'NIST Standard Reference Database Number 69' [online] available from < https://webbook.nist.gov/chemistry/> [18 Nov. 2018].
[147] Vander Wal RL, Weiland KJ. Laser-Induced Incandescence: Development and Characterization Towards a Measurement of Soot-Volume Fraction. Appl Phys B 1994;59(4):445–52.
[148] Verdier A, Marrero Santiago J, Vandel A, Saengkaew S, Cabot G, Grehan G, et al. Experimental Study of Local Flame Structures and Fuel Droplet Properties of a Spray Jet Flame. Proc Combust Inst 2017;36(2):2595–602.
[149] Wegner B, Maltsev A, Schneider C, Sadiki A, Dreizler A, Janicka J. Assessment of Unsteady RANS in Predicting Swirl Flow Instability Based on LES and Experiments. Int J Heat Fluid Flow 2004;25(3):528–36.
[150] Westbrook CK, Dryer FL. Simplified Reaction Mechanisms for the Oxidation of Hydrocarbon Fuels in Flames. Combust Sci Technol 1981;27(1–2):31–43.
[151] Widmann JF, Charagundla SR, and Presser G (1999) *Benchmark Experimental Database for Multiphase Combustion Model Input and Validation: Characterization of the Inlet Combustion Air* [online] available from < https://www.nist.gov/publications/benchmark-experimental-database-multiphase-combustion-model-input-and-validation-1> [22 Jan. 2018].
[152] Widmann J, Presser C, Papadopolous G. 'Benchmark Database for Input and Validation of Spray Combustion Models - Inlet Air Characterization'. In *39th Aerospace Sciences Meeting and Exhibit*. held 8-11 January 2001 at Reno, Nevada, U.S.A. ed. by American Institute of Aeronautics and Astronautics (2001).
[153] Widmann J, Rao Charagundla S, and Presser C. 'Benchmark Spray Combustion Data for Code Validation'. In *38th Aerospace Sciences Meeting and Exhibit*. held 10-13 January 2000 at Reno, Nevada, U.S.A. ed. by American Institute of Aeronautics and Astronautics (2000).
[154] Widmann JF, Presser C. A Benchmark Experimental Database for Multiphase Combustion Model Input and Validation. Combust Flame 2002;129(1–2):47–86.
[155] Yuan R. Measurements in swirl-stabilised spray flames at blow-off. Cambridge: University of Cambridge; 2015. PhD thesis.
[156] Zhu S, Roekaerts D, Pozarlik A, van der Meer T. Eulerian–Lagrangian RANS Model Simulations of the NIST Turbulent Methanol Spray Flame. Combust Sci Technol 2015;187(7):1110–38.